KfK 4632
November 1989

Optimization of a Single Sphere Albedo System Using ^{3}He Counters for the Measurement of Neutron Dose Equivalent Rates and the Field Calibration of Personnel Albedo Neutron Dosimeters

M. I. Al-Jarallah
Hauptabteilung Sicherheit

Kernforschungszentrum Karlsruhe

KERNFORSCHUNGSZENTRUM KARLSRUHE

Hauptabteilung Sicherheit

KfK 4632

OPTIMIZATION OF A SINGLE SPHERE ALBEDO SYSTEM USING ^{3}He COUNTERS FOR THE MEASUREMENT OF NEUTRON DOSE EQUIVALENT RATES AND THE FIELD CALIBRATION OF PERSONNEL ALBEDO NEUTRON DOSIMETERS

MOHAMMAD I. AL-JARALLAH [1]

1) On leave from the King Fahd University of Petroleum and Minerals, Physics Department, Dharan, Saudi Arabia

Kernforschungszentrum Karlsruhe GmbH, Karlsruhe

Kernforschungszentrum Karlsruhe GmbH
Postfach 3640, 7500 Karlsruhe 1

ISSN 0303-4003

ABSTRACT

The laboratory type of an active single sphere albedo dosementer system using three ^{3}He proportional counters in a polyethylene sphere for the measurement of neutron dose equivalent rates and the field calibration of personnel neutron dosemeters was optimized with respect to the detectormoderator combination by means of calibration exposures. One detector is located in the centre of the sphere to measure the neutron dose equivalent rate and the other two detectors near the moderator surface, in order to simulate the response of the albedo neutron detector and the thermal neutron detector as it was done in the passive albedo personnel dosemeter using thermoluminescent detectors in a boron loaded plastic capsule. The response of the detectors to neutrons of different energies in the range between thermal and 14 MeV neutrons was investigated for various moderatorabsorber combinations. Comparison was made between the system response and the response of the passive detector system. After completion the active system could be used for comprehensive neutron field measurements in radiation protection. By means of a microprocessor the linear combination of the three detector readings gives energy independent readings of the neutron dose equivalent rate, the absorbed dose rate and the neutron flux density at particle accelerators and nuclear facilities.

Optimierung eines Einkugelalbedodosimetersystems mit ^{3}He-Zählrohren zur Messung der Neutronen-Äquivalentleistung und zur Feldkalibrierung von Albedopersonendosimetern.

Zusammenfassung

Der Laboraufbau eines aktiven Einkugelalbedo-dosimetersystems mit 3 ^{3}He-Zählrohren in einer Moderatorkugel zur Messung der Neutronen-Äquivalentdosisleistung und zur Feldkalibrierung Neutronenpersonendosimetern wurde hinsichtlich der von Detektor-Moderatoranordnung unter Verwendung von Kalibrier-bestrahlungen optimiert. Ein Detektor zur Messung der Äquivalentdosisleistung ist im Zentrum der Kugel ange-ordnet und die anderen Detektoren an der Moderatoroberfläche, um wie beim passiven Albedopersonendosimeter mit Thermolumi-neszenzdetektoren in einer Borplastikkapselung das An-sprechvermögen des Albedoneutronendetektors und des thermi-schen Neutronendetektors anzunähern. Das Ansprechvermögen der Detektoren wurde unter Verwendung unterschiedlicher Modera-tor-Absorber-kombinationen mit Neutronen unterschiedlicher Energien im Bereich thermischer bis 14 MeV Neutronen untersucht. Verglichen wurde das Ansprechvermögen des Systems mit dem Ansprechvermögen des passiven Detektorsystems. Nach Fertigstellung könnte das aktive System zu umfassenden Neutronenfeldmessungen im Strahlenschutz herangezogen werden. Bei Einsatz eines Mikroprozessors erhält man über die Linearkombination der 3 Detektoranzeigen eine energie-unabhängige Anzeige der Neutronen-Äquivalentdosisleistung, der Energiedosisleistung und der Neutronenflußdichte an Teil-chenbeschleunigern und kerntechnischen Anlagen.

CONTENTS

1. Introduction:

One of the more important problems of radiation protection is the assessment of the dose equivalent to organs of the body resulting from the exposure to neutrons. The practical measurement of neutrons presents special problems. As they are uncharged particles, their detection is based on the products of their interaction with matter. The major difficulties arise from a number of factors, namely (a) the wide range of neutron energies, from a few hundredths of an electron volt to several hundred million electron volts, (b) the irregular variation of neutron interaction cross-sections with energy, particularly in the intermediate energy range where sharp resonance peaks are found, (c) the presence of other types of radiation, especially gamma rays, and (d) the fact that no detector can mimic exactly the artificial factors which are introduced to provide the dose equivalent. All these give rise to problems in the development of techniques of neutron monitoring, design of monitoring instruments and the assessment of dose equivalents resulting from exposure to neutrons alone or to mixed radiation fields [1].

The main sources of neutrons are sealed radionuclide sources, nuclear reactors and particle accelerators (including neutron generators).

Neutrons are encountered in the enrichment of fissile materials and in the processing of spent fuels. Neutron sources are also widely used in the medicine and industry. Neutron monitoring is therefore a subject of increasing general interest and considerable attention is being paid to the development of improved techniques and methods for neutron monitoring [1].

The neutron detection methods could be divided into two main categories; dynamic and passive. In the dynamic methods, active detectors are used to obtain an immediate indication of neutron dose equivalent or fluence. In the passive methods, the type of detectors used to store the information and require some form of "development" or readout procedure to provide the dose reading. This kind of detectors like thermoluminescent detectors TLD's is usually called passive detectors.

Very frequently the neutron dose equivalent received by individual in mixed neutron/photon fields is estimated on the basis of measurement with neutron survey meters (active detectors). These consist of cylindrically or spherically shaped polyethylene (PE) moderators of linear dimension of about 2Ø cm to 3Ø cm diameter. The moderated neutrons are detected by thermal neutron detectors, such as proportional counters filled with BF_3 or ^3He gas. Boron or cadmium absorbers are usually used in the moderator to modify the response to be less energy dependent. However, it was found that the readings of these

survey meters are highly energy dependent and are also dependent on the direction of incident neutrons as shown in Fig.1 and Fig. 2. Although the energy and angular response of survey meters are tolerated because they are, usually, detecting neutrons all over the energy range of interest, however, there is still the need for developing a neutron survey meters with less energy and angular dependence. Survey instruments and pocket alarm neutron dosimeters using proportional counters are still under development in Europe and the United State [3].

Also passive detectors in neutron personnel dosimetry, whether thermoluminescence detectors [TLD's] or solid state nuclear track detectors [SSNTD's] are in a similar way energy and angular dependent in their readings, beside being dependent on other factors [3]. Mainly because of energy dependence, in particular, albedo dosimeters require calibration in the actual field location in order to get an accurate reading of the neutron dose equivalent. Spectrometers and multisphere detectors have been used in the past to provide the calibration factors for albedo dosimeters in stray radiation fields [4]. These techniques generally allow an estimate of the neutron fluence spectrum and thus a calculation of the dose equivalent and all relevant data for stray neutron field. It is, however, questionable whether the accurate measurement of only dose equivalent justifies the use of spectrometers. With respect to a simple standard calibration technique it is also doubtful whether

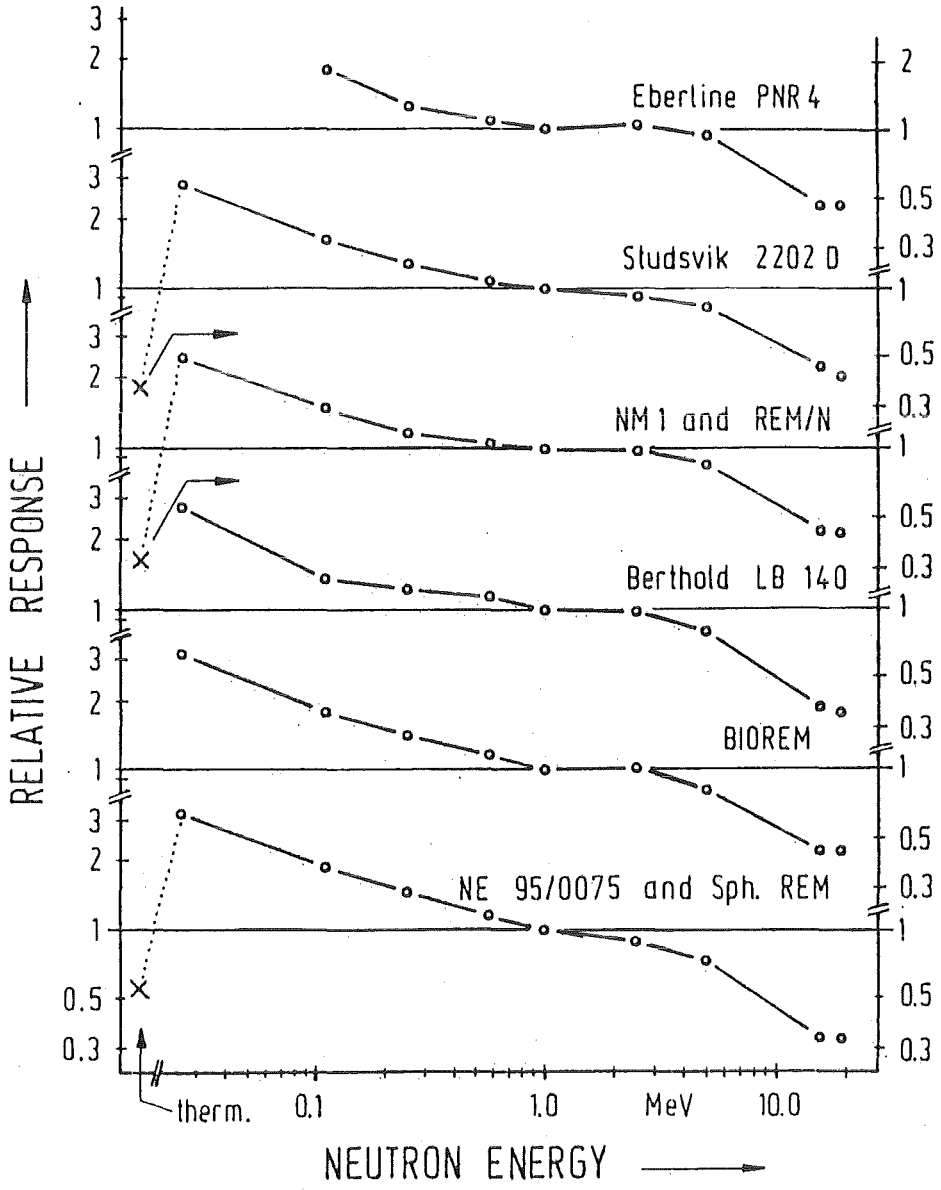

FIG.1 RELATIVE DOSE EQUIVALENT RESPONSE OF VARIOUS NEUTRON SURVEY METERS VERSUS NEUTRON ENERGY. THE VALUES ARE NORMALIZED TO 1 AT 1 MeV[2].

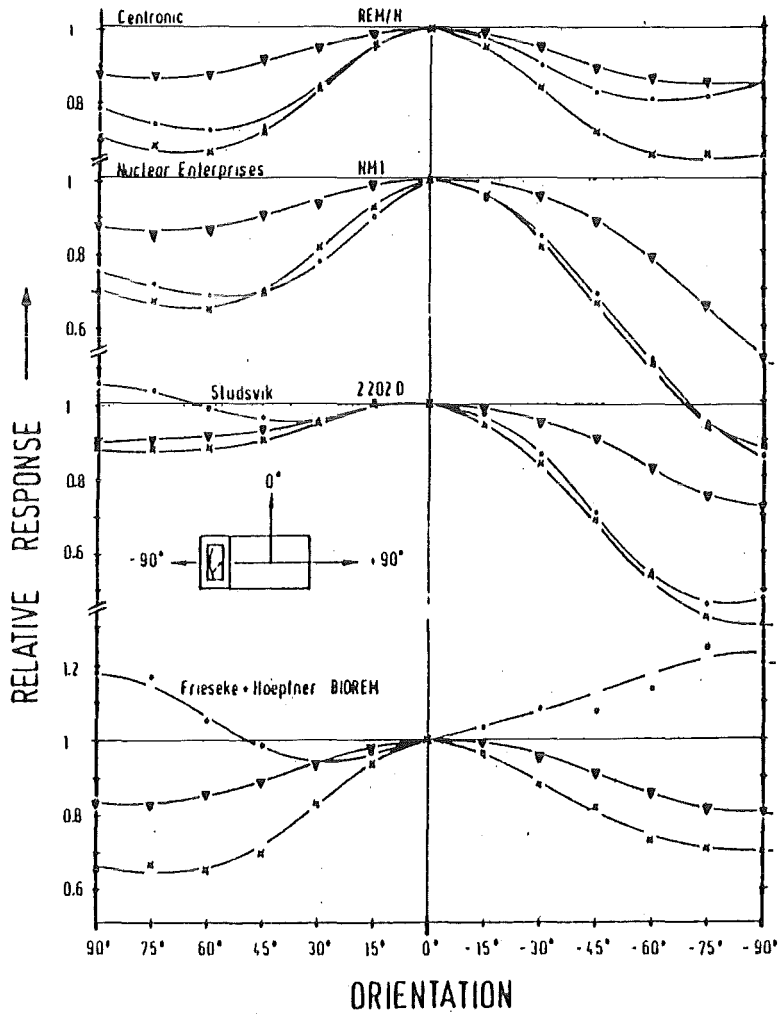

FIG. 2 DEPENDENCE OF THE RESPONSE OF VARIOUS NEUTRON SURVEY METERS ON THE INSTRUMENT ORIENTATION WITH RESPECT TO THE INCOMING NEUTRONS AT THE ENERGIES OF 110 KeV (.), 1 MeV (x) AND 15.5 MeV (V). THE DEFINITION OF THE ANGLE IS SKETCHED[2].

for example, the multisphere technique should be applied [5].

The main objective of developing an active system using only one sphere are twofold; first to measure neutron dose equivalent with good accuracy and minimum energy dependence, and second, to use it as a reference dosimeter for a quick calibration of passive albedo dosimeters in the radiation field around nuclear facilities and accelerators.

The Single Sphere Albedo System to be developed here will include three ^{3}He proportional counters in a polyethylene sphere. One counter placed in the centre of the sphere measures the dose equivalent similar to a "rem counter". The other two counters are placed near the surface of the sphere and simulate the albedo dosimeter. One is surrounded by a boron-loaded tube from all directions except the front in order to measure mainly thermal neutrons incident from the radiation field only [Fig.5, shieldings No.4 and No.9]. The other counter is covered in front with a boron loaded disk to measure mainly albedo neutrons backscattered from the sphere [Fig.5, shielding No.1].

The evaluation technique makes use of the linear superposition of the three detector readings using an on-line computer program in order to allow the immediate estimation of neutron fluence, absorbed dose, dose equivalent and quality factor, all of which are practically independent of the neutron energy. It was assumed that the system provides a minimum angular dependence.

2. Single Sphere Albedo Technique(*)

Neutrons entering the human body are moderated and back scattered, thus creating a neutron fluence at the body surface, especially in the thermal and intermediate energy range. The back scattered neutrons from the human body called albedo neutrons, can be detected by a thermal neutron detector placed on the body [1]. This process of neutron measurement is applied in the albedo neutron dosimetry.

The ratio of the thermal albedo neutron fluence to the incident neutron fluence approaches unity for thermal neutrons and low energy neutrons, but falls to about Ø.1 at higher energies of about 1MeV. In addition, the neutron fluence-to-dose equivalent conversion factor is much more smaller for fast neutrons than for thermal or intermediate energy neutrons. As a consequence of these two factors the response of albedo dosemeters, in general, is highly energy dependent and cannot be affected significantly by the dosimeter design. The dose equivalent response defined as the ratio of albedo detector reading to the neutron dose equivalent is about 1ØØ times greater for thermal neutrons than for neutrons of energy of about 1MeV. Nevertheless, it has been shown that by careful design of the

---

(*) Section 2 is taken, mainly, from ref.2 and ref.7.

albedo neutron dosemeter and by the adoption of an appropriate technique for field and read out calibration, it is possible to measure the neutron dose equivalent in practical situations with adequate accuracy[6].

The design of a universal albedo neutron dosemeter makes use of pairs of detectors, for instance, of TLD-600/TLD-700 pairs, one pair behind the "window" for the measurement of field thermal neutrons, the other inside a boron-loaded capsule for the measurement of albedo thermal neutrons. The albedo neutron windows, which differ in size according to the TLD system, have been optimised and designed separately for TLD cards manufactured by Alnor, Harshaw, Panasonic, Teledyne, and Vinten in order to minimise the detector-to-body distance effect. The universal albedo neutron dosimeter is the official neutron personnel dosimeter in the Federal Republic of Germany which is applied in all kinds of stray neutron fields. In the case of moderated neutron sources it provides an internal correction of the location dependent change of the neutron calibration factor on the basis of measured field calibration curves [6].

Piesch and Burgkhardt [4] have developed a technique for field calibration of albedo dosemeters. The technique makes use of at least three TL detectors, one in the centre of a 30cm polyethylene (PE) sphere and two within an albedo dosemeter located on the surface of the sphere. The single sphere albedo system in its old design is shown diagrammatically in figure 3

which also shows the fluence response of the TLD's in the sphere and the albedo dosemeters on the sphere.

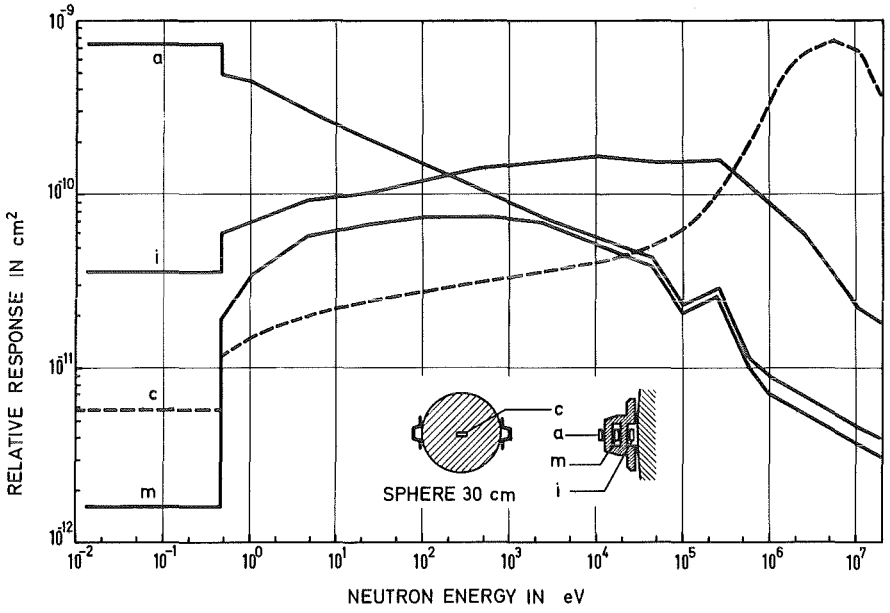

FIG.3 FLUENCE RESPONSE FUNCTIONS OF ^{6}LIF DETECTORS USED IN THE POLYETHYLENE SPHERE OF 30 CM DIAMETER AND IN THE KARLSRUHE ALBEDO DOSIMETER [1].

To reduce the energy response of the central detector (c) in the sphere, two independent approaches have been made in the past.

In the first approach [3], the detector reading of the sphere has been separated into fraction of thermal, epithermal and fast neutrons and then corrected for energy dependence by using constant response factors for the energy range of thermal and epithermal neutrons and the actual response for fast neutrons found by means of an energy parameter.

In a new approach independent of the former one, the linear superposition of the readout of three detectors k=a, i,c directly allows the estimation of the neutron fluence, absorbed dose, dose equivalent and quality factor almost independent of the neutron energy:

$$\phi = k_1.\underline{M}(a) + k_2.\underline{M}(i) + k_3.\underline{M}(c) \qquad (2.1)$$

$$D = k_4.\underline{M}(a) + k_5.\underline{M}(i) + k_6.\underline{M}(c) \qquad (2\text{-}2)$$

$$H_{MADE} = k_7.\underline{M}(a) + k_8.\underline{M}(i) + k_4.\underline{M}(c) \qquad (2\text{-}3)$$

where M(k) is the reading of the detector with k=a,i,c and k_i being constant calibration factors with i=1 to 9. D is the absorbed dose and H_{MADE} is the maximum dose equivalent, according to the recommendation of ICRP 21.

Knowing the fluence response functions $R_{\phi,k}(E)=M(k)/\phi(E)$ energy independence is realized by using Eq. (2-1) and to obtain

TABLE 1 CALIBRATION FACTORS, K_i OF THE SINGLE SPHERE ALBEDO TECHNIQUE USING THE LINEAR COMBINATION OF THREE DETECTOR READINGS

Neutron detector	least square fit facors k_i for				
	(10^{-6}cm^{-2})	D (10^{-2}mGy)	H_{MADE} (10^{-1}mSv)	H*(10) (10^{-1}mSv)	HE (10^{-1}mSv)
a	$k_1 = 1.1$	$k_4 = 0.62$	$k_7 = 0.16$	$k_{13} = 13$	$k_{10} = 0.084$
i	$k_2 = 5.9$	$k_5 = 1.4$	$k_8 = -1.2$	$k_{14} = -1.5$	$k_{11} = -0.9$
c	$k_3 = 1.4$	$k_6 = 8.8$	$k_9 = 8.3$	$k_{15} = 8.3$	$k_{12} = 5.8$

the best approximation, the constant factors k_i have been evaluated by a least square fit using a system of 200 equations for different energies from thermal to 20 MeV neutrons. The corresponding response functions for absorbed dose $R_{d,k(E)}$ and dose equivalent, $R_{h,k(E)}$ have been obtained from $R_{\phi,k(E)}$ taking into account the recommended nuetron fluence-to-absorbed dose and neutron fluence to dose equivalent conversion factors for the maximal dose equivalent H_{MADE} tabulated for discrete energies in ICRP 21.

The result of this approach is presented in Table 1 and Fig.4 (dashed lines) for the estimation of the neutron fluence, absorbed dose, dose equivalent and the quality factor $Q=H_{MADE}/D$. In the case of a neutron spectrum, the energy response becomes smoother compared with that of monoenergetic neutrons. This is shown in Fig.4 (solid lines) where the neutron energy can be interpreted as a mean energy of a neutron spectrum having a Gaussian distribution with a full width at half maximum value which is similar to that of an unmoderated fission spectrum. At each energy the response is the mean response for this spectrum.

For ϕ and D, the energy dependence does not exceed $\pm$ 20% in the neutron energy range of interest. With respect to dose equivalent, the linear superposition reduces energy dependence of

the 3Ø cm sphere from a factor of 4 to ± 5Ø% for monoenergetic neutrons and to about ± 3Ø% in stray neutron fields. Using calibration factors presented in Table 1, the single sphere albedo technique results in energy independence for effective dose equivalent H_E within ± 2Ø% but for ambient dose equivalent H*(10) [7,8] within ± 42% only [5]. With respect to the estimation of the neutron dose equivalent, the single sphere albedo system eliminates the over-response of the 3Ø cm sphere at epithermal and fast neutron energies as the under-response for thermal neutrons. This technique has been widely used in the Federal Republic of Germany for field calibrations and measurements in research and power reactors and other establishments [1].

The previous advantages of the single sphere albedo system brought the idea of replacing the passive TL detectors by active neutron detectors, and reducing the moderator size to get an appropriate survey instrument of minimum energy and angular dependence. This survey instrument is not available so far, and this is the subject of the present research.

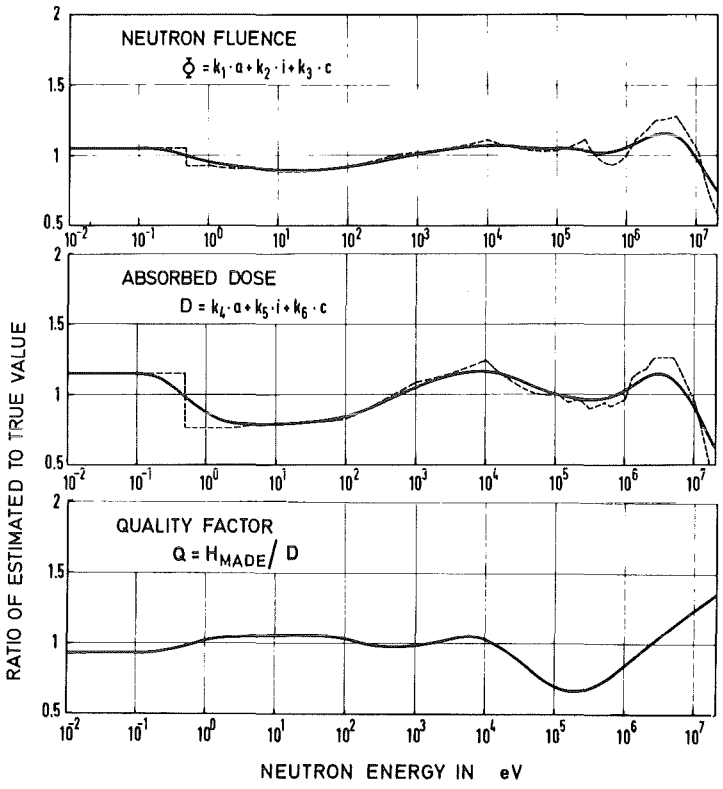

FIG. 4a : LINEAR SUPERPOSITION OF THREE DETECTOR READINGS a, i AND c FOR THE ESTIMATION OF NEUTRON FLUENCE Ø, ABSORBED DOSE D, DOSE EQUIVALENT H, AND QUALITY FACTOR Q AS A FUNCTION OF NEUTRON ENERGY BASED ON THE RESPONSE FUNCTION.

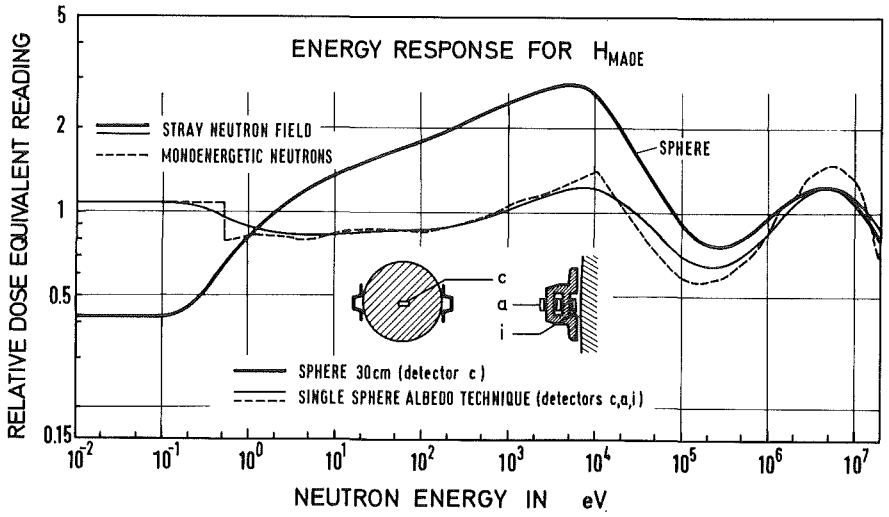

FIG. 4b : RELATIVE DOSE EQUIVALENT RESPONSE H_{MADE} OF A 30cm POLYETHYLENE SPHERE AND OF THE SINGLE SPHERE ALBEDO SYSTEM USING THREE DETECTOR READINGS.

3. Equipments

TABLE 2 SPECIFICATIONS OF THE NEUTRON COUNTERS AND PASSIVE DETECTORS

Counter Type	^{3}He Thompson Ø.5 NH 1/1 K	BF^{3} 2Ø122 LND, Inc.	BF_{3} N.Wood G-5-1.
Thermal neutron efficiency ($C.S^{-1}.n.cm^{2}.S$)	Ø.5		
Overall length (mm)	63	14Ø	155
Effective length (mm)	1Ø	23.5	51
External diameter (mm)	1Ø	12.8	12.8
Operating Voltage (V)	155Ø	16ØØ	16ØØ-18ØØ
Gas pressure (pascal)	$8 \times 1Ø^{5}$	$Ø.73 \times 1Ø^{5}$	$Ø.8 \times 1Ø^{5}$
Passive detectors	TLD-6ØØ and TLD-7ØØ, Harshow		
Evaluation in	ALNOR automatic readout system.		

*Boron Absorbers:

Different boron shieldings [5Ø% by weight boron powder mixed with plastic glue: UHU plus end fast 3ØØ] were used to shield the surface detectors in the positions 1--->9 of the PE Spheres, as shown in Fig.5.

Experiments have been performed using ^{3}He counters in positions No.1 to No.9.(see Fig. 5 and Table 2)

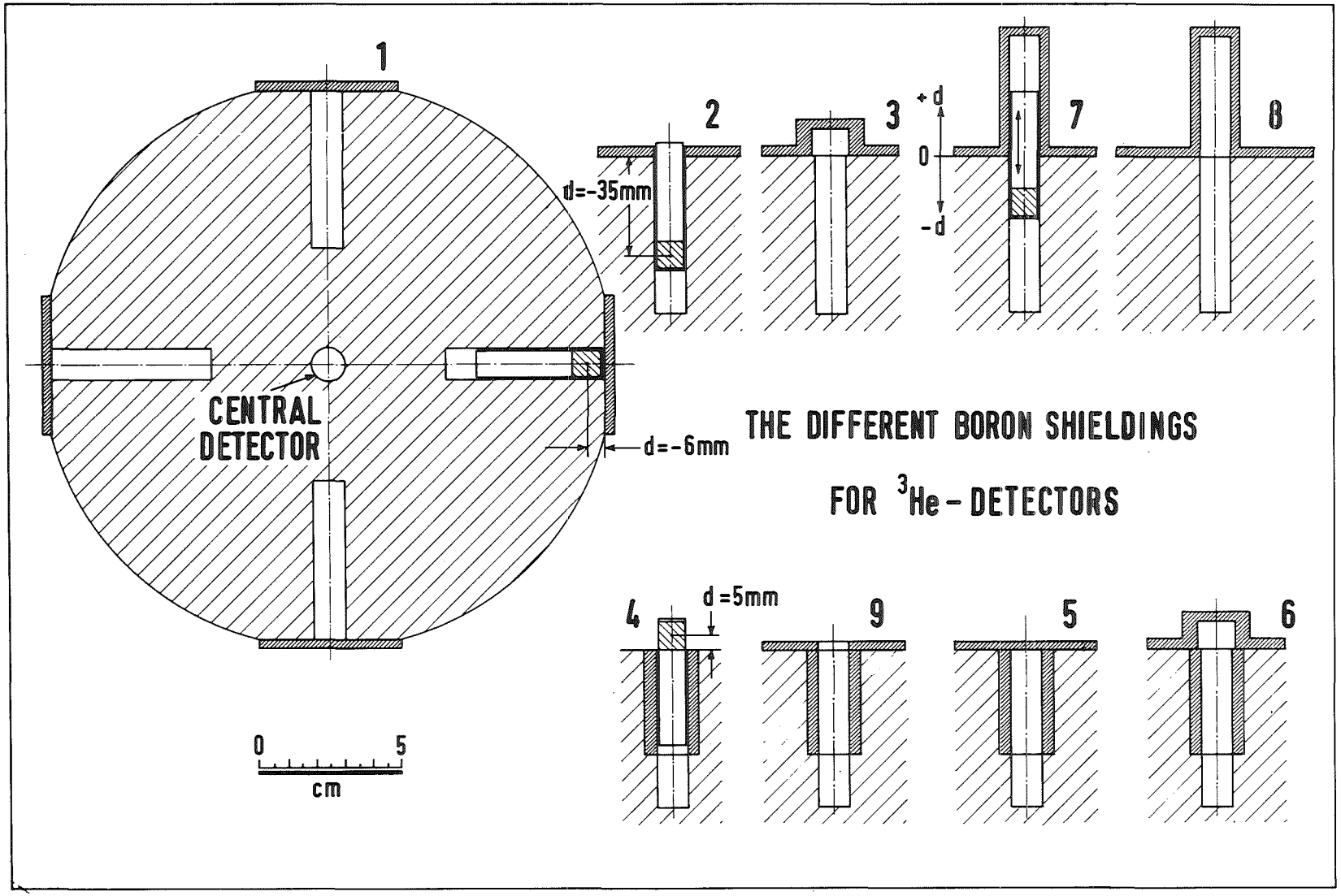

FIG. 5 : THE CONFIGURATIONS OF THE "WHITE" PE SPHERES.

4. Experiments and Evaluation Technique

All preliminary measurements were done using a 30cm "black" [with graphite] polyethylene sphere and four small ^{3}He counters delivered by Thomson which were available at the time. One of the detectors was placed in the centre of the sphere (c). The other three were placed near the surface. They were accomodated in concentric holes; one in front [0°] to face neutron beams and two at the two sides [90° and 270°] as shown in figure 6. A fourth hole was made on the back of the sphere to accomodate a fifth detector [180°] [Figure 6].

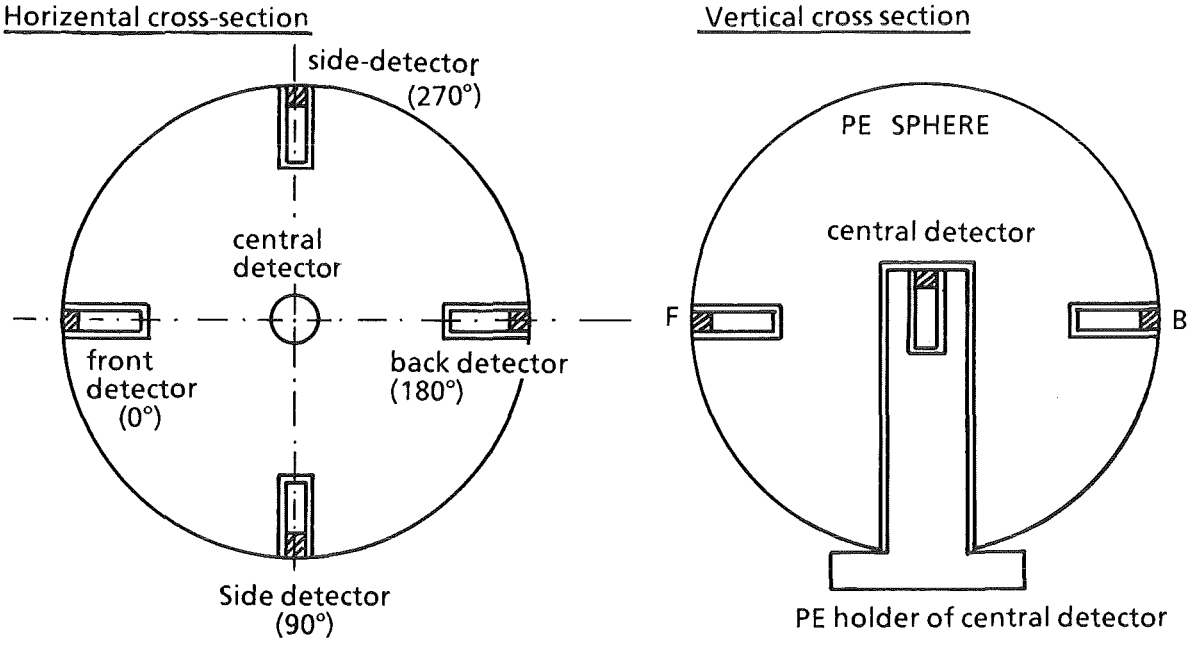

FIG.6 THE POSITIONS OF THE FIVE DETECTORS IN THE "BLACK" PE SPHERE

Later, "white" PE sphere [without graphite] was used instead of the black one to exclude any change in the carbon content of the PE sphere [$N(C_2H_4)$]. Due to the heavy mass of the 3Øcm sphere of 14 kg, spheres of smaller diameters were used namely 25cm and 2Ø cm diameter weight about 8 and 4 kg, respectively.

The use of the first 3Øcm black PE sphere with the original configuration showed difficulties in fixing and changing the surface detectors positions at different depths. Therefore different configuration in the PE spheres was made for holding the detectors near the surface anabling easy positioning and fixing of the detectors. This was achieved by making four PE cylinders to hold the detectors in positions as shown in Figure 7. Holes of similar size were made in each of the three different diameters white PE spheres at Ø°, 9Ø°, 18Ø° and 27Ø° positions to accomodate these PE cylinders [figure 8].

The new configuration made it easy and possible to position the detectors on the surface at desired depths from inside or outside [see figure 28] and minimize holes in the PE spheres [i.e. decrease loss of moderator].

The central detector was held in the centere of PE sphere with PE cylinder holder.

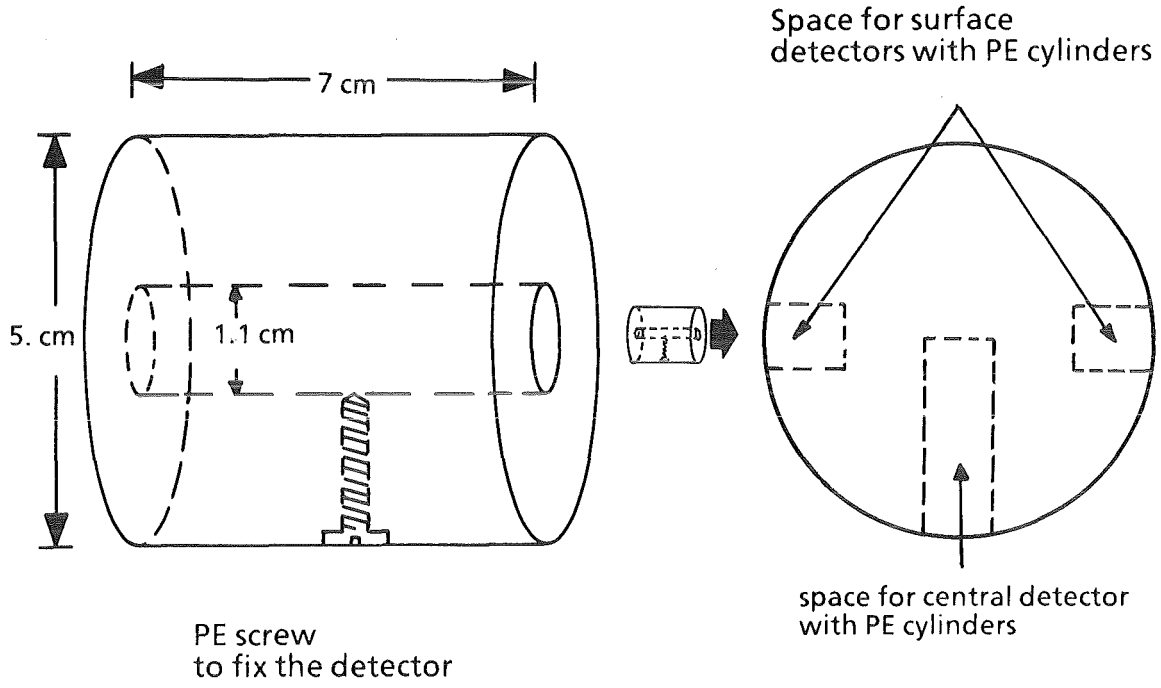

FIG.7 THE POLYETHELYNE CYLINDER FIG.8 CROSS-SECTION IN THE "WHITE" PE SPHERES, SHOWING THE POSITIONS OF DETECTORS

To measure the response of the direct thermal neutron component [Ra] incident from the radiation field [section 1], three PE cylinders of similar size [figure 7] was made. The detector holes in the cylinders were surrounded with boron loaded plastic tubes of 3 mm thickness and 37 mm long [figure 5 No.4]. This was done to absorb thermalized neutrons in the PE sphere from being detected. It was estimated that the thermalized neutrons in the PE sphere which may enter from the

back uncovered end of the boron tubes is minimal, since the effective part of the ^{3}He counter lies in front [see figure 5 No.4]

Nine different boron loaded plastic shieldings were used for the measurements of the albedo response Ri and the thermal neutron response Ra as shown in figure 5. Shielding Nos. 1,2,3,7, and 8 used in measuring Ri. Shieldings No. 1 and 3 used to exclude direct thermal neutrons. Shielding No. 2 was used only in fast neutron field with negligible thermal neutron component when the detector showing outside PE sphere. Shielding No.7 and 8 were used to exclude direct thermal neutrons when checking thermal neutron sensitivity in the thermal beam at EIR for detector positions deeper than 1Ømm in the sphere. Shielding Nos.4,5,6, and 9 used in Ra measurements together with the boron tube mentioned earlier. The boron ring in shielding No.9 used to exclude the detection of albedo neutrons when the detectors are showing outside the PE sphere. Shielding No.5 and 6 were used when checking the response of the detectors to fast neutrons to exclude detecting thermalized neutrons from the surrounding.

4.1 Experiments with Cf-252 Neutrons:

All preliminary measurements to investigate the response of the surface and central detectors in different polyethylene spheres were done in the KfK calibration hall using the Cf-252

fission neutron source of known activity. The detector source height from the ground was 1.25m in most cases at distances of 1.5m or 2m apart from the source. The contribution of back scattered neutrons from ground and wall in the wooden calibration hall of the size 8m x 12m x 8m were significant. Therefore, other measurements were carried out at a height of four meters above floor to minimize back scattered neutrons from the ground. Measurements with and without shadow cone were also done to get accurate reading without back scattering.

The new calibration hall of the KfK with its modern gamma exposure facility using C_S-137 sources of different strengths was also utilized to investigate the sensitivity of different proportional counters to gamma rays, since gamma rays always accompany neutrons.

4.2 Experiments with monoenergetic neutrons at the PTB

The most critical test of any dose or dose equivalent devices is the use of monoenergetic neutrons, since the use of neutron spectrum average out extreme values of the response. However, this does not happen with monoenergetic neutrons especially if the contribution of back scattered neutrons from the surrounding environment is low and can be ignored. Therefore the facility in the National Institute for Physics and Technology [Physikalisch-Technische Bundesanstalt (PTB)] was utilized to test our system with monoenergetic fast neutrons of different energies.

The institute is well staffed and equipped for accurate measurements and calibration. Two particle accelerators [HVEC Van de Graaff and a TCC Cyclotron of variable energy] are used in the production of monenergetic neutrons at different energies. The amount of wall scattered neutrons is kept low, as a large experimental hall [area 3Øm-24m, height 14m,] is available with the neutron producing target close to the geometrical centre. All stands and constructional material in the hall are light weight especially in the vicinity.

The energy and angular dependence of our system using the three different sphere sizes were inspected by varying both, depths (d) of the surface detectors in the PE spheres and the energy of fast neutrons of Ø.144, Ø.25, Ø.57, 1.2, 2.5, 5.5 and 14.8 MeV. The target to sphere distance was fixed at 1.5m distance.

4.3 Experiment with Thermal Neutrons at the EIR

The experimental test of our system with monoenergetic fast neutrons was done at the PTB. Since sources of intermedite neutron energies between Ø.4eV and 1ØØ keV of reasonable flux are not easily available, therefore, the sensitivity of our system in the energy range will be found, as usual, by calculation. So the only experiment to inspect our system in the low energy range is the use of thermal neutrons, which are very important from the practical point of view because they contribute in every neutron field.

Since the PTB reactor was under renovation and could not be used, arrangement was made with the Swiss Federal Institute for Reactor Research [Eidenossisches Institute fur Reakorforschung EIR] to utilize their pool research reactor in Wurenlingen to test our system.

Since the thermal neutron beam flux and its cross-sectional area were not known exactly by the reactor authority, therefore, simple measurements were carried out to inspect it. Five bare ^{3}He counters were fixed on top of each other at a distance of 3cm from each other with the lowest counter at a height of 1Ø5 cm above the ground which is considered to be the centre of the thermal neutron beam. Then two scannings were done, forward and backward, and the count rate of each detector was typed every two seconds using a scanner speed of Ø.366 cm/sec. Then another scannings, forward and backward, were carried out with the four counters brought down keeping the central counter in position unchanged at a height of 1Ø5cm. These measurements revealed that the thermal neutron beam cross section was less than the cross sectional area of the 2Øcm PE sphere, and also not uniform over the whole cross-section. (Figure 9). Therefore, two scanning were carried out at two heightsl.03m andl.07m in order to cover the whole sphere. To exclude fast neutron components from the reactor beam, each scanning was repeated twice, one without putting any absorber in front of the neutron beam, and in other scanning, a 1 mm cadimum filter was used in front of the reactor beam. The difference of the two measurements made, without Cd

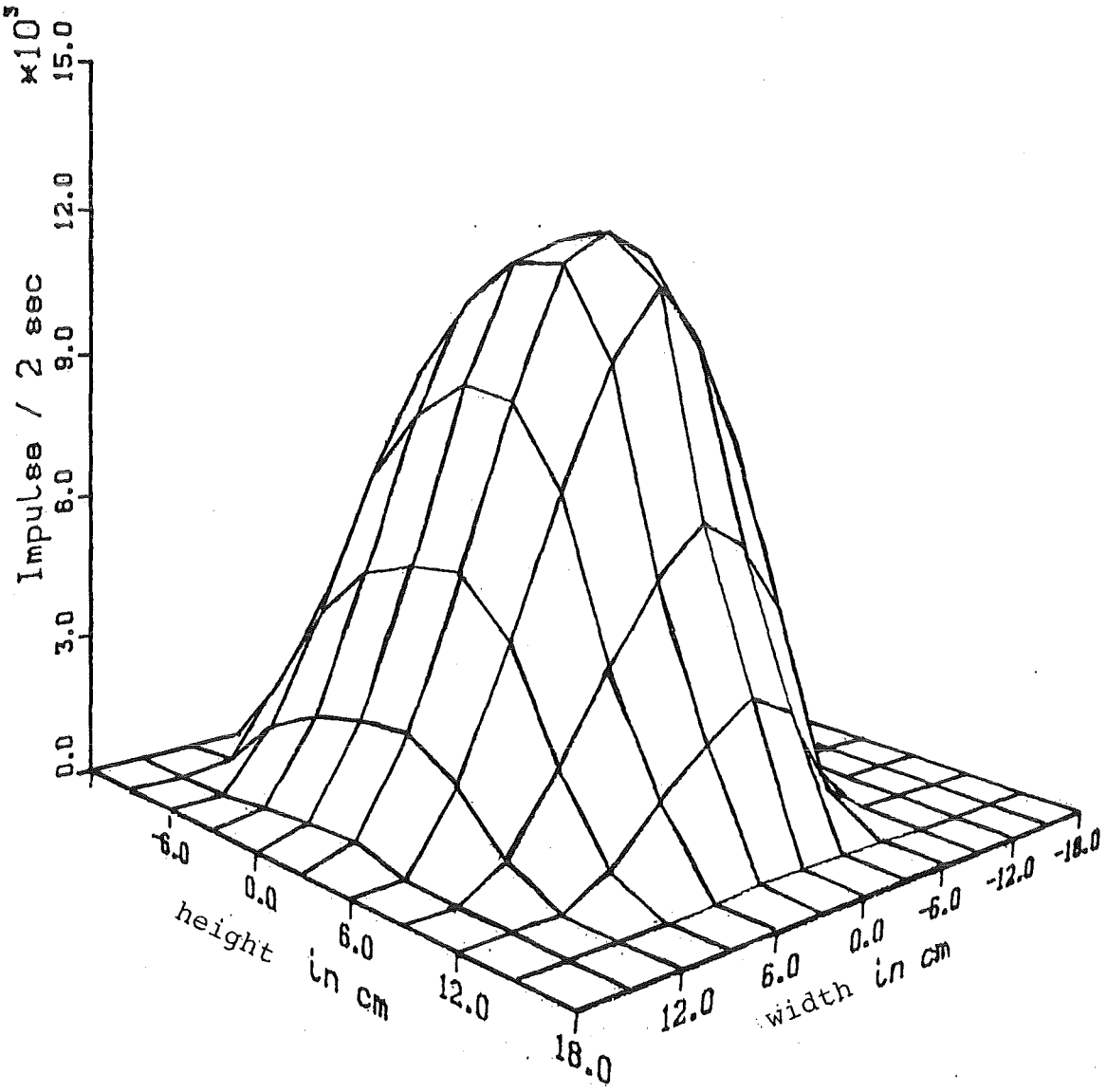

Fig. 9 INTENSITY PROFILE OF THE THERMAL NEUTRON BEAM AT EIR.

and with Cd, gives neutron component below the Cd cutoff [i.e. below Ø.4eV, see figure 9].

Finally, the normalization of measurements were done based on the calibration with Cf-252 neutrons and the difference in energy response for thermal neutrons.

4.4 Experiments in Stray Neutron Fields at DKFZ:

Preliminary experiments were carried out to do neutron measurements in the stray neutron of a cylotron. The Heidelberg Cyclotron Lab in the German Cancer Research Center [Deutsches Krebs-Forschungs Zentrum: DKFZ] was chosen because the reading ratio of the thermal detector and the albedo detector [i.e. a/i] varies significantly over the different locations of the irradiation hall [figure 10]. The lab houses a compact cyclotron for therapy irradiations which can give neutron beams with an average neutron energy of 8.5 MeV[Fig.11]. In this lab, the average neutron energy varies significantly over the different experimental hall locations due to neutrons back scattering from ground, walls and roof. This is the reason for the significant variation of a/i mentioned earlier.

Fixed detectors position in the PE spheres of the diameters 3Ø cm and 2Ø cm was chosen for both Ri and Ra measurements [for detectors (i) a depth of d=-6 mm and for detector (a) a depth of d=5 mm was used, see figure 5] for easy comparison of different measurements.

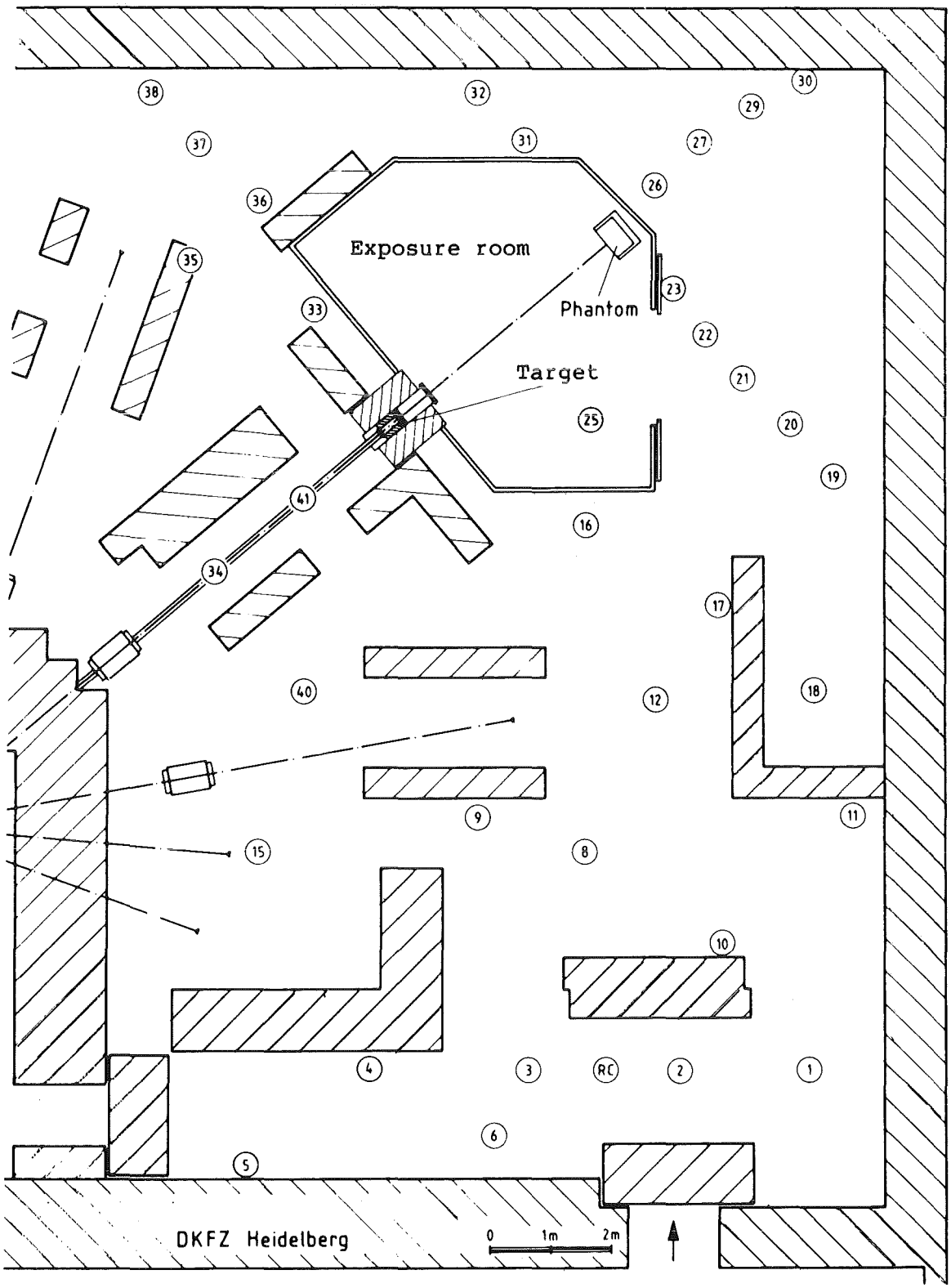

FIG.10 SCHEMATIC DIAGRAM OF THE ACCELERATOR, FACILITY IN THE DKFZ HEIDELBERG SHOWING THE NEUTRON BEAM LINE AND THE DIFFERENT LAB'S LOCATIONS.

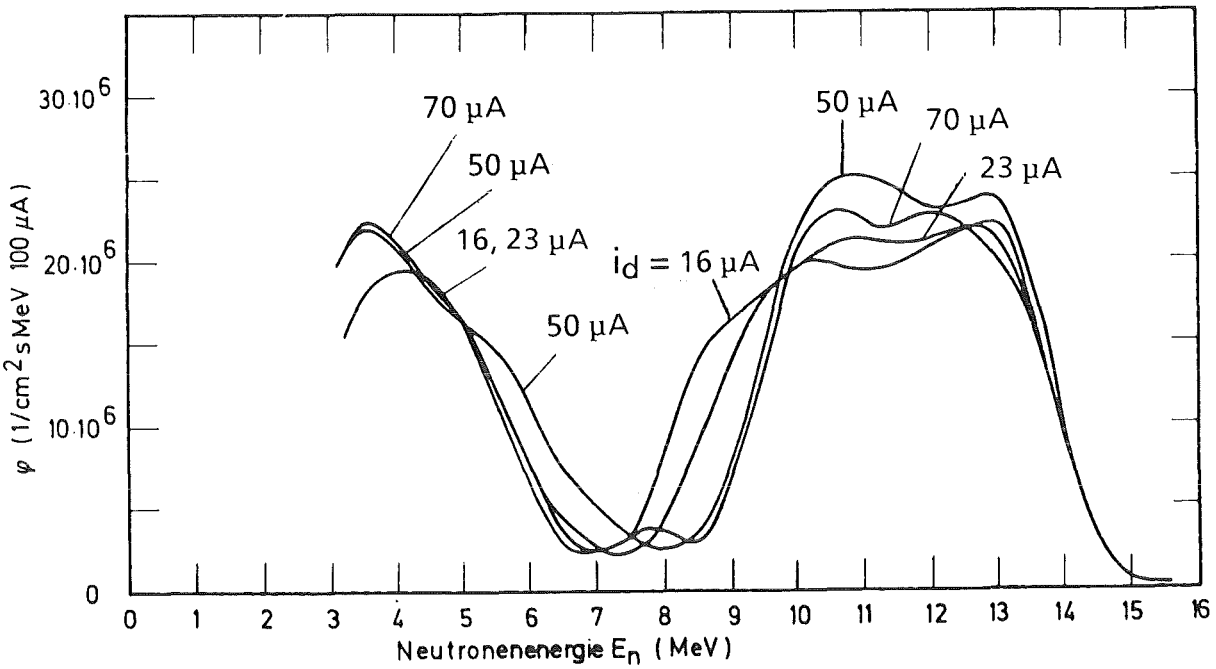

FIG.11 THE NEUTRON ENERGY SPECTRA OF HEIDELBERG COMPACT CYCLOTRON: (d,n) REACTION [9].

At the same time, passive measurements were carried out at different locations using the single sphere albedo technique with thermoluminescent detectors [TL detectors : ^{6}LiF and ^{7}LiF] for comparison of passive detector measurements [Ri, Ra and Rc] with the active detector measurements of the system. In the past passive detector measurements were carried out in the same centre using the single sphere albedo technique [6] with a slightly different design of the albedo dosimeter than that was used in our experiment. It was found that Ri/Rc values are highly correlated to Ri/Ra values.

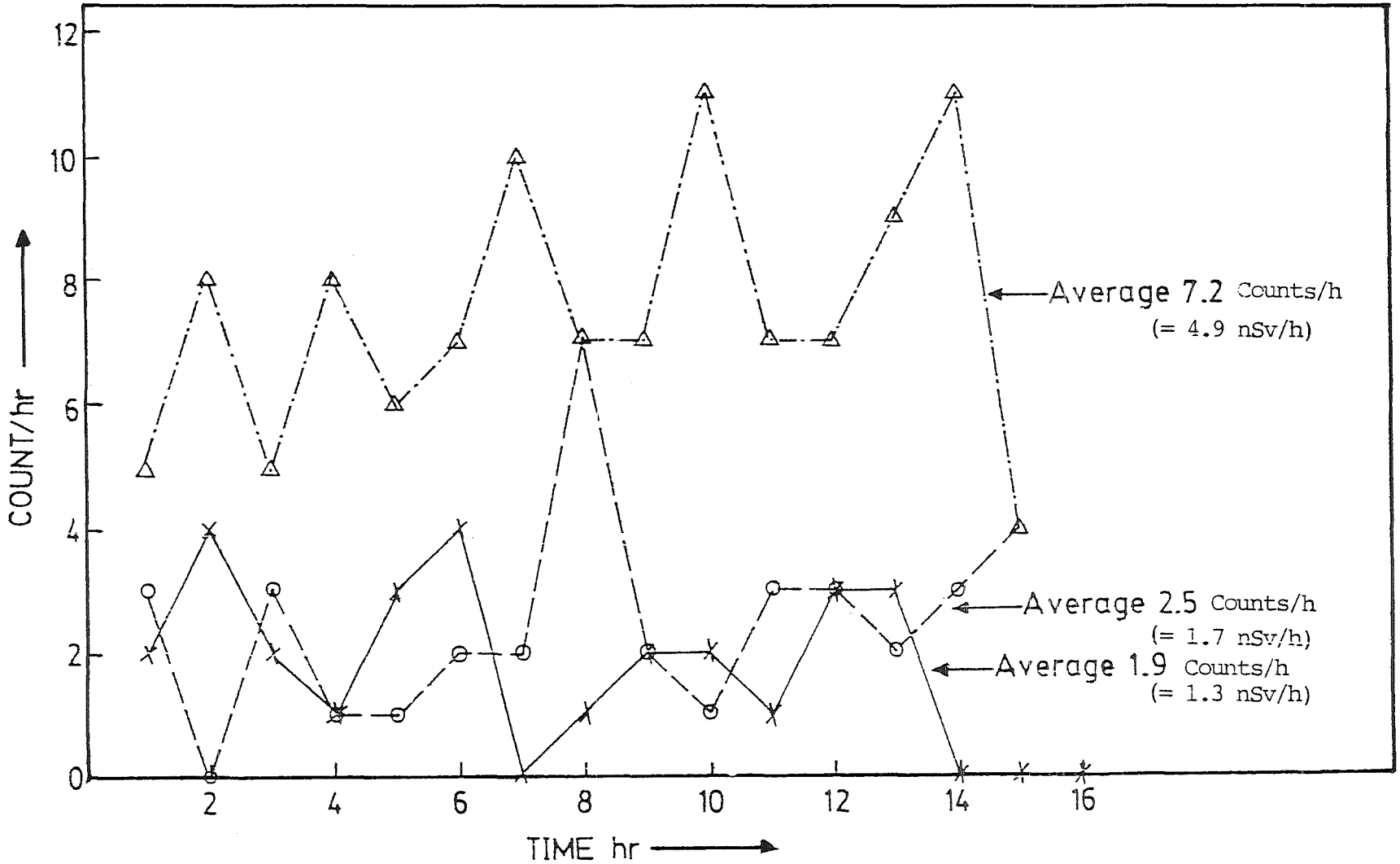

FIG.12 OVER NIGHT BACKGROUND MEASUREMENTS FOR THREE ^{3}HE COUNTERS

5. Evaluation of Experimental Results

5.1 Detectors' Characteristics:

The first step in constructing the active detectors system was to choose a proper active detector. Thereare few pre-requisites which should be met by the detectors to suit the proposed system:

- Small size to simulate passive detectors used in the single sphere albedo technique.
- Good n-γ discrimination, to exclude errors due to the presence of γ-rays in stray neutron fields.
- Low spurious count rate, good stability and high neutron sensitivity to enable measuring dose rates with good reproducibility and accuracy.

Proportional counters are the most widely used detectors for neutron dosimetry for many reasons [see ref.2]. Three kinds of proportional counters were considered: two BF_3 and one ^3He [section 3]. Their different characteristics were studied. It was found that the BF_3 counters are superior in terms of their n-γ discrimination as expected. However, ^3He detector is better in terms of stability, low spurious count rate, and is also smaller in size [active volume less than 1 cm^3]. These advantages made ^3He detectors our choice.

Experimental investigation of these detectors reveals the following: Figure 12 shows overnight measurements with ^3He counters [counts starts from channel 25Ø onward and total 1Ø24

channels] which disclose that two of the three ^{3}He detectors have been found to be very stable and the average 1-3 counts per hour, which is equivalent to Ø.7 --> 2 nSv/hr could be due to real neutrons from cosmic rays [i.e. natural neutron background] However, some ^{3}He detectors which showed higher and unstable spurious count rates were excluded.

The used BF_3 counters showed much higher spurious count rates in overnight measurements [figure 13] with higher fluctuation [some time higher than expected by the statistical uncertainty].

Figures 14 and 15 show the photon, neutron and n+γ spectra of the BF_3 detectors type N.WOOD and type LND. respectivily. It can be noticed that there is no problem in the photon discrimination with BF_3 detectors even at very high gamma dose rates. Even at a γ-dose rate of 77mSv/hr, the γ-spectrum end before channel 15Ø while the neutron spectrum starts after channel 3ØØ as shown in figure 16. This is expected for BF_3 detectors due to the high alpha and ^{7}Li energies which are produced in the detection reaction $^{1Ø}B\ (n,\alpha)^{7}Li$.

^{3}He has higher neutron absorption cross-section than boron-1Ø however, its low Q-value in the neutron reaction makes γ-discrimination more difficult than that for a BF_3 tube [10]. Figure 17 shows the neutron, photon and n+γ spectra for the ^{3}He detector. The interference in the neutron measurements

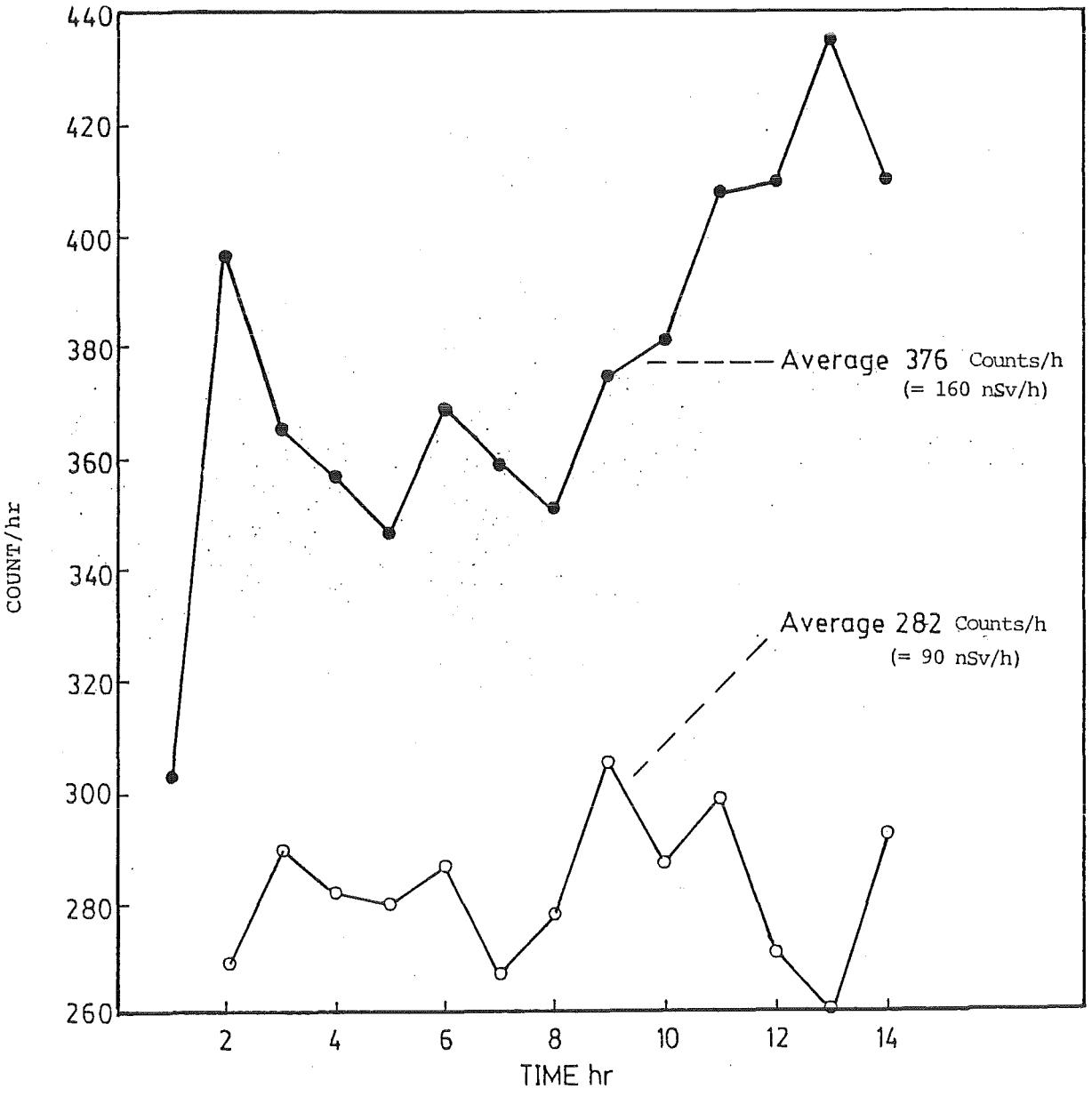

FIG.13 OVER NIGHT MEASUREMENTS FOR TWO BF_3 LND COUNTERS.

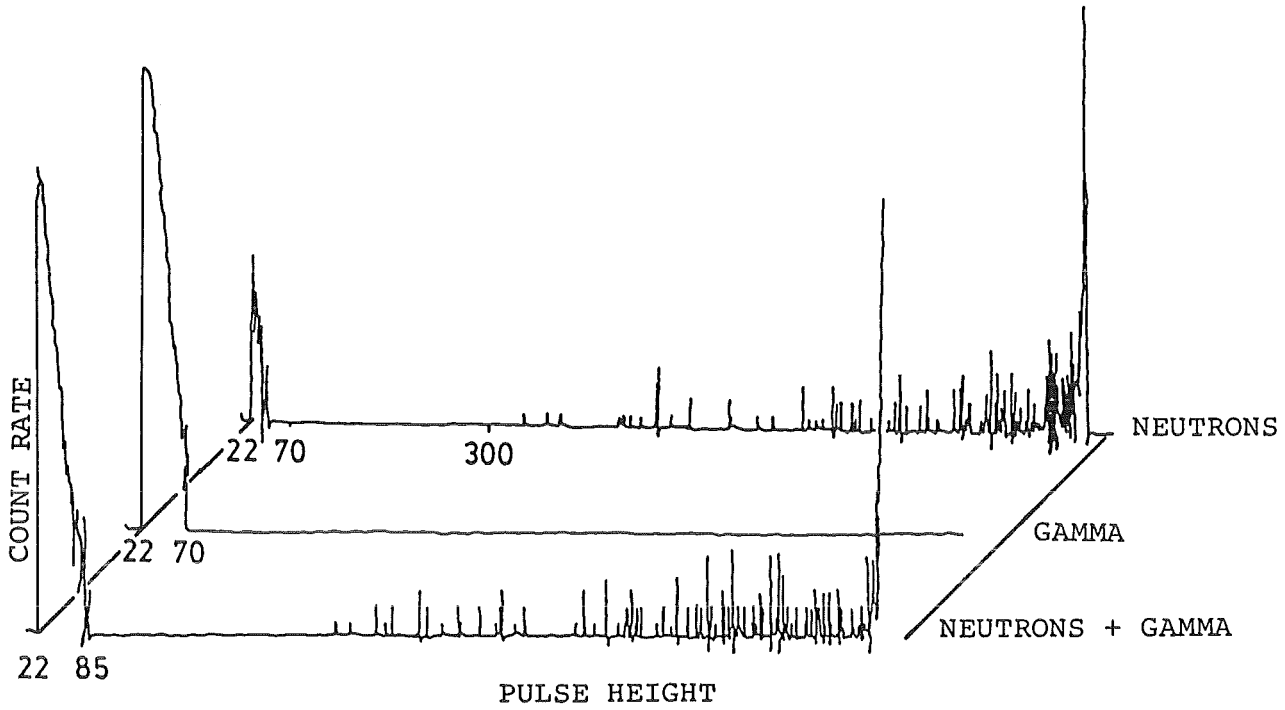

FIG. 14 : PULSE HEIGHT SPECTRA OF PROPORTIONAL COUNTER, BF_3 N.WOOD, FOR n[1.4 mSv/h], γ [4.4 mSv/h] and n + γ .

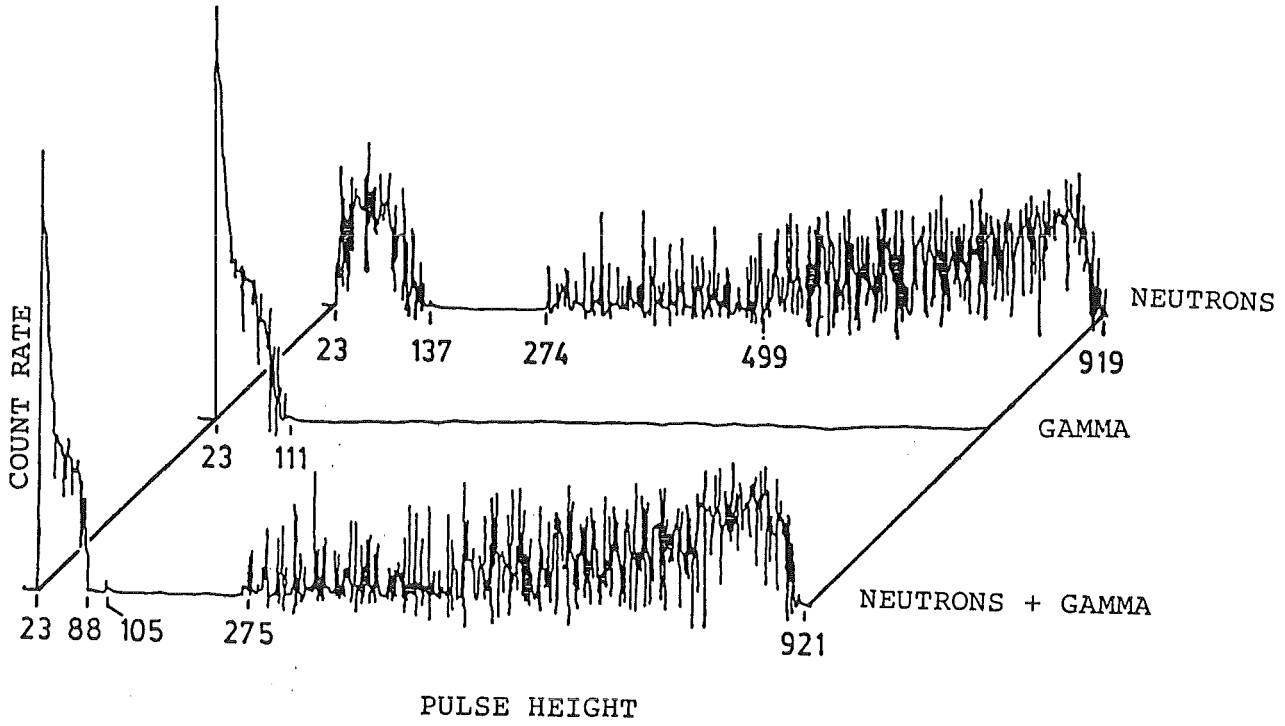

FIG. 15 : PULSE HEIGHT SPECTRA OF PROPORTIONAL COUNTER, BF_3 LND, FOR n[1.4 mSv/h], γ [4.4 mSv/h] and n + γ .

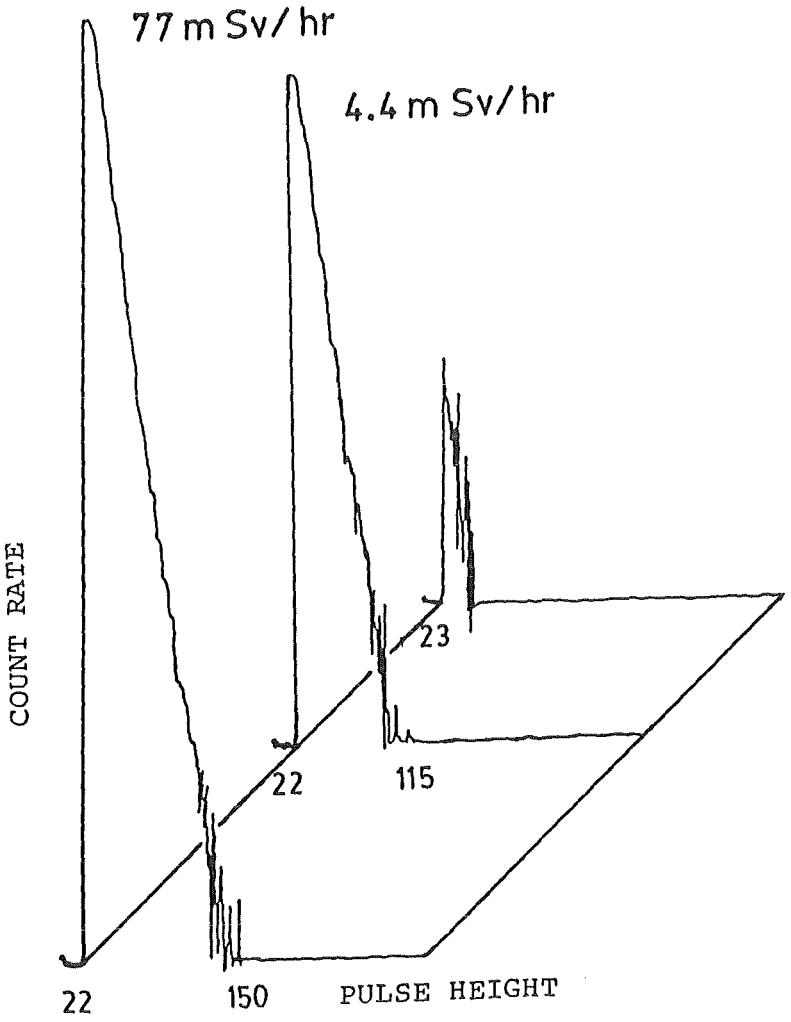

FIG. 16 GAMMA SPECTRA OF PROPORTIONAL COUNTER, BF_3 N.WOOD, FOR DIFFERENT γ DOSE RATES.

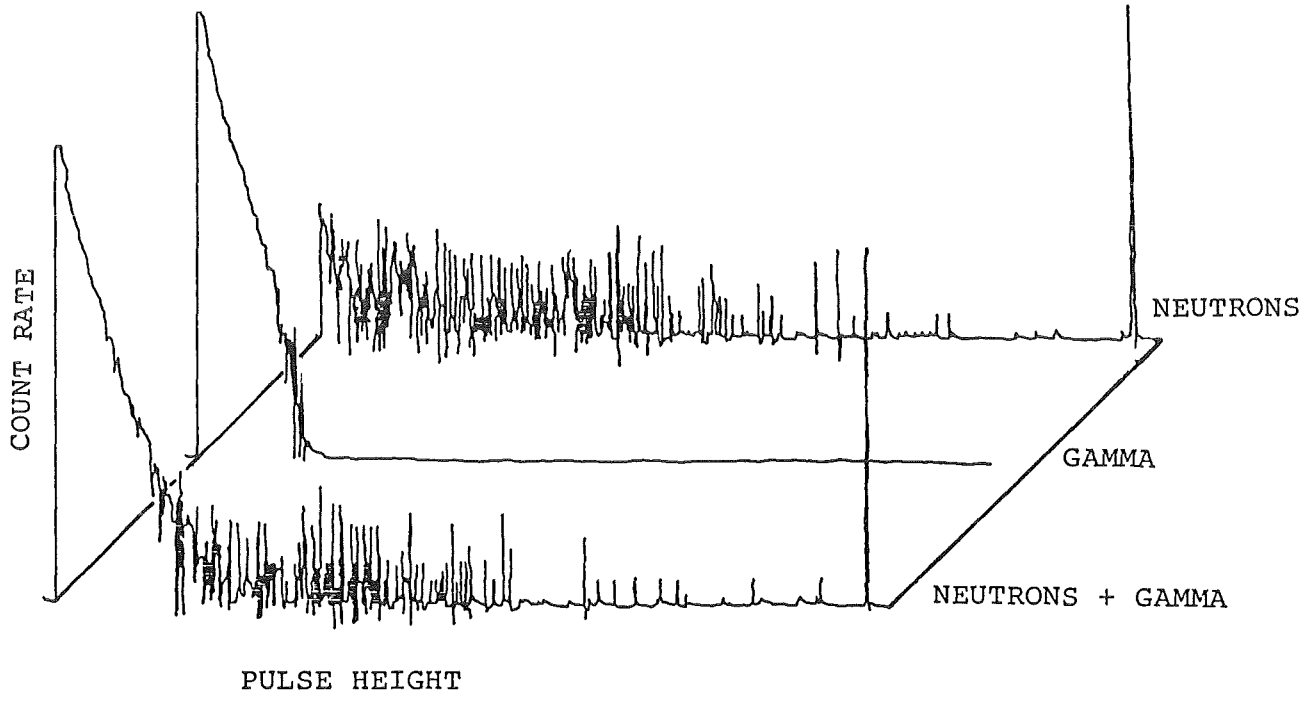

FIG. 17 PULSE HEIGHT SPECTRA OF PROPORTIONAL COUNTER, ^{3}He THOMSON, FOR n[1.4 mSv/h], γ [17.2 mSv/h] and n + γ.

is apparent if counts starts from low channels using a low pre-amplifier discrimination level. Therefore neutron counts have to start from higher channels by increasing the pre-amplifier discrimination level.

Figures 18 and 19 show the variation of neutron and gamma count rates with bias voltage for ^{3}He detectors when counts starts from channel one, and figure 2Ø shows this variation when the counts starts from channel one and channel 324 also.

The gamma spectrum expands with the increase of γ-dose rate as shown in figure 21.

Increasing the detector bias voltage from 155Ø volts, the recommended working voltage, to 165Ø volts expands gamma spectrum by one fold as shown in figure 22.

The pre-amplifier discrimination level were set at 73ØmV so that counts starts from channel 25Ø, and it was tested that when detectors are in position in the PE sphere, photon dose rates up to 1ØØ mSv/h gives minimal count rates which is equivalent to spurious count rates.

It was found experimentaly, using the Cf-252 source, that by starting the counts from channel 25Ø the loss in the neutron counts was 35% and when starting the counts from channel 324, the loss in neutron sensitivity raised to 56% [see figure 23].

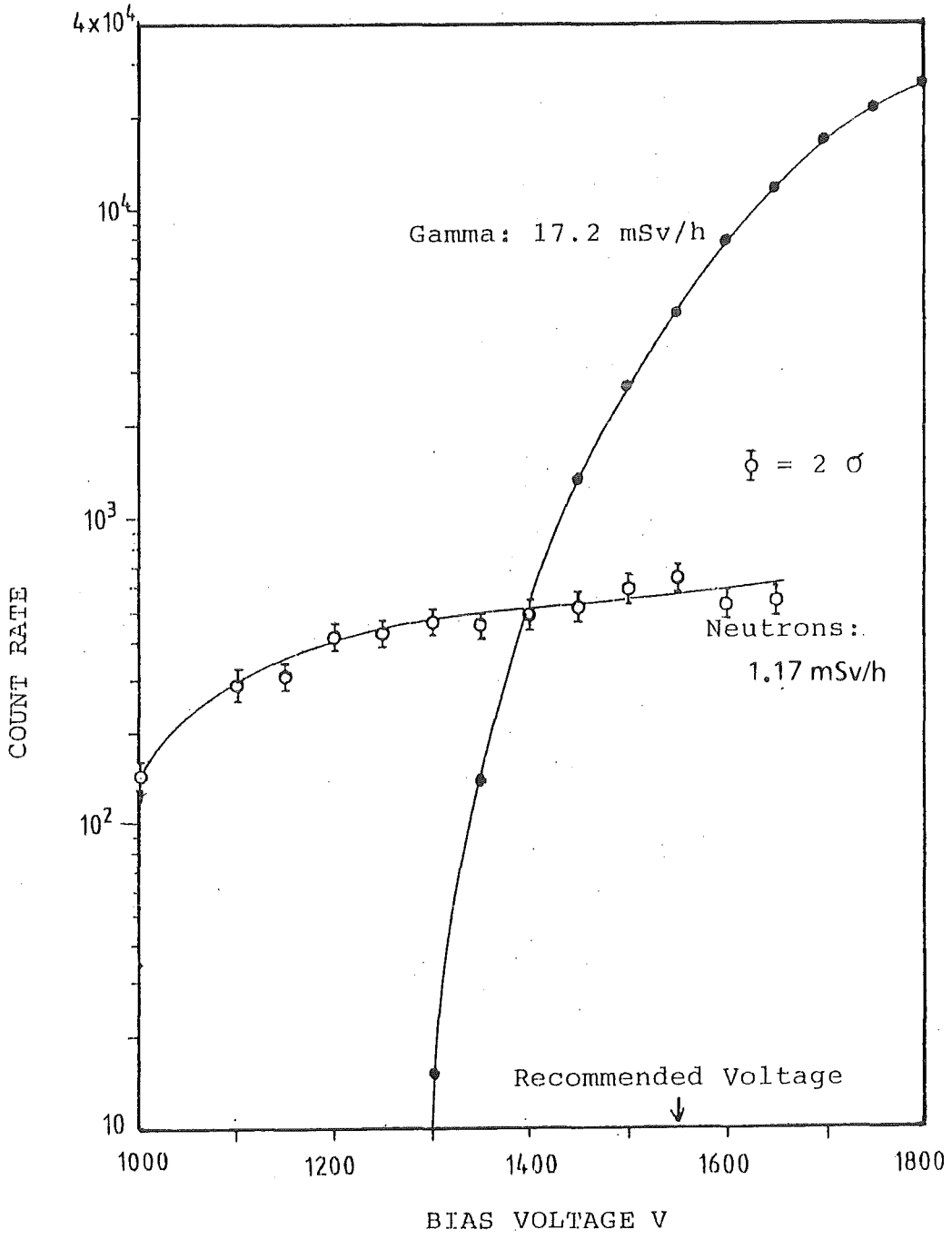

FIG. 18 NEUTRON AND GAMMA TOTAL COUNT RATES (CHANNEL 1 TO 1024) OF PROPORTIONAL COUNTER ^{3}He THOMSON, VERSUS BIAS VOLTAGE.

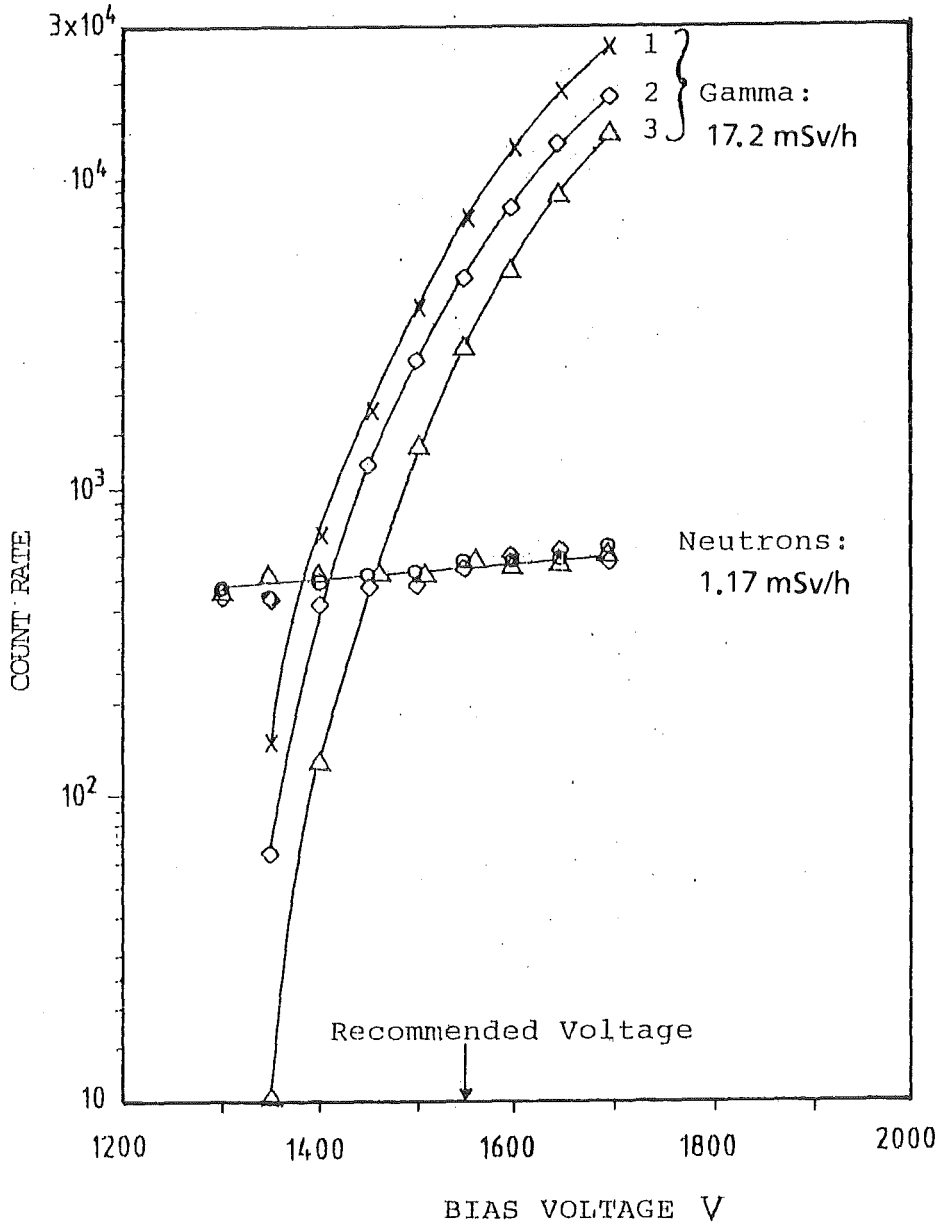

FIG. 19 NEUTRON AND GAMMA TOTAL COUNT RATES OF THREE PROPORTIONAL COUNTERS, ^{3}He THOMSON, VERSUS BIAS VOLTAGE.

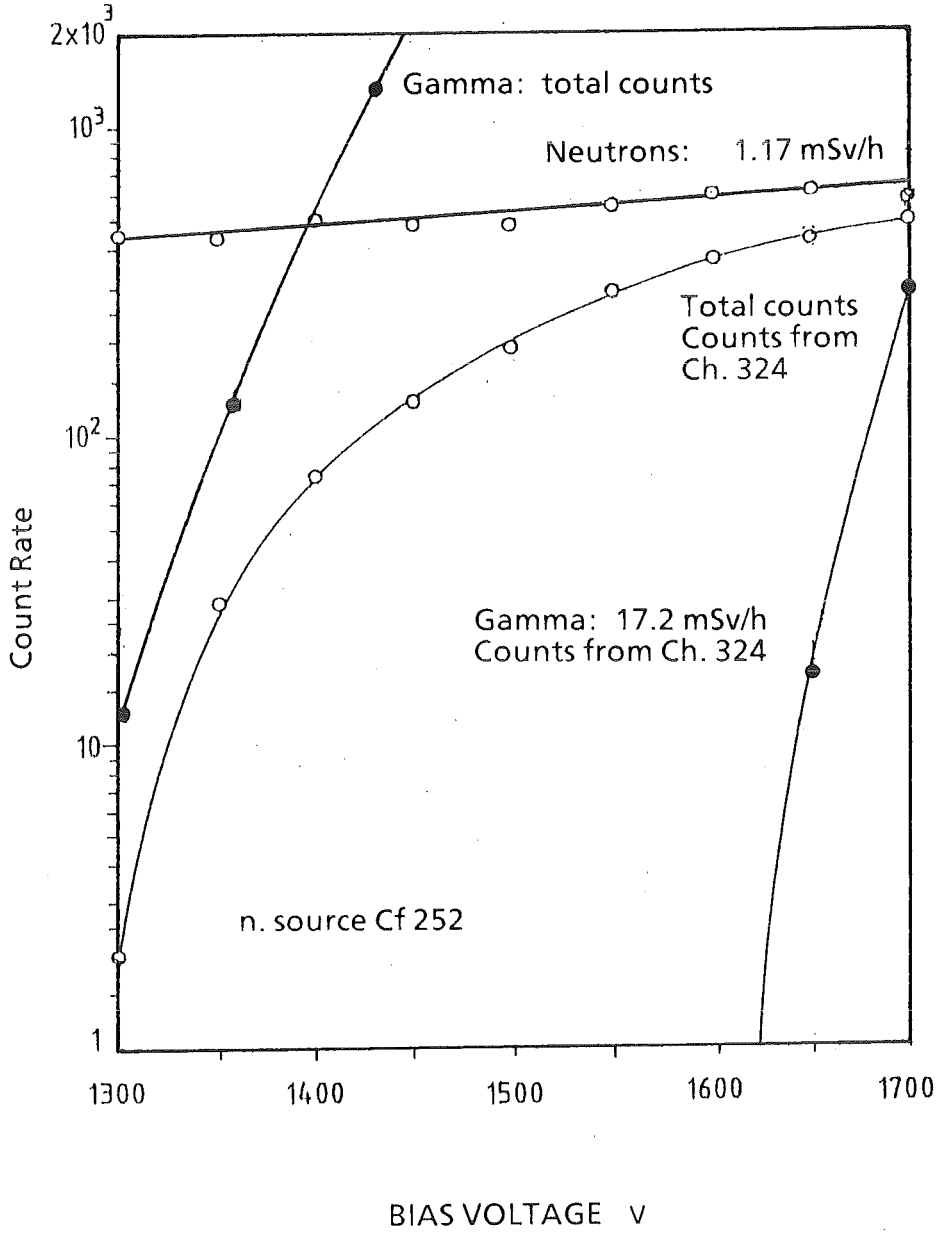

FIG.20 NEUTRON AND GAMMA COUNT RATES OF TWO PROPORTIONAL COUNTERS, ^{3}He THOMSON VERSUS BIAS VOLTAGE, FOR TOTAL COUNTS AND COUNTS FROM CHANNEL 324.

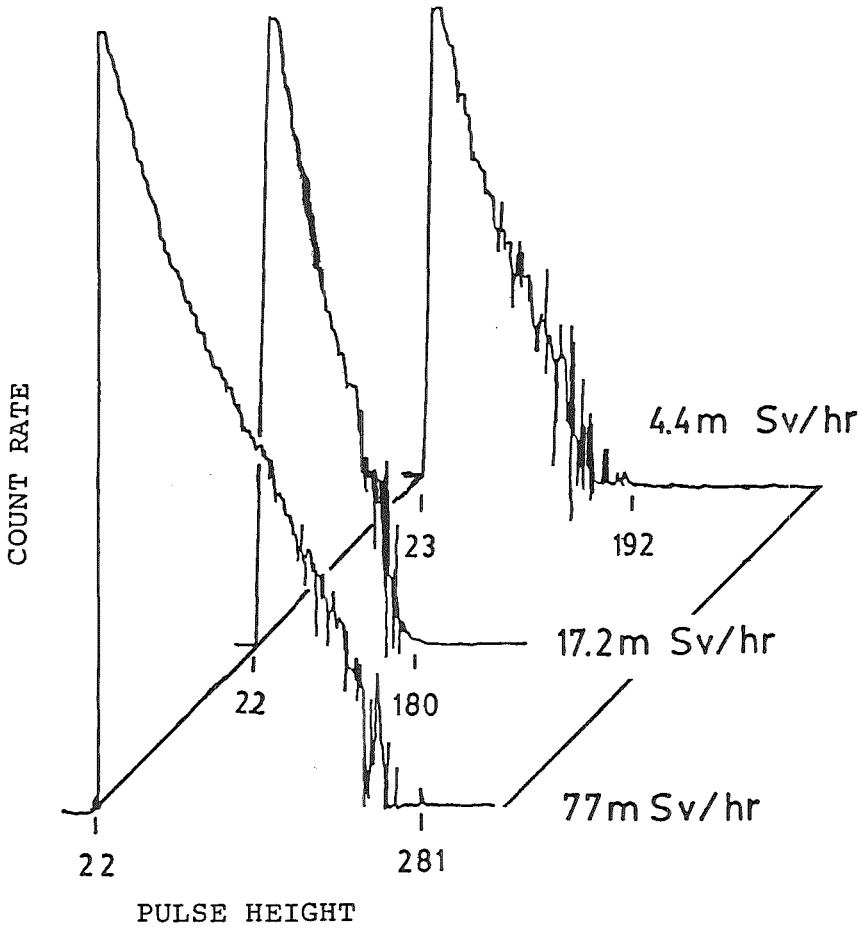

FIG. 21 GAMMA SPECTRA OF PROPORTIONAL COUNTER, ^{3}He THOMSON, FOR DIFFERENT γ DOSE RATES AT THE BIAS VOLTAGE 1550 V.

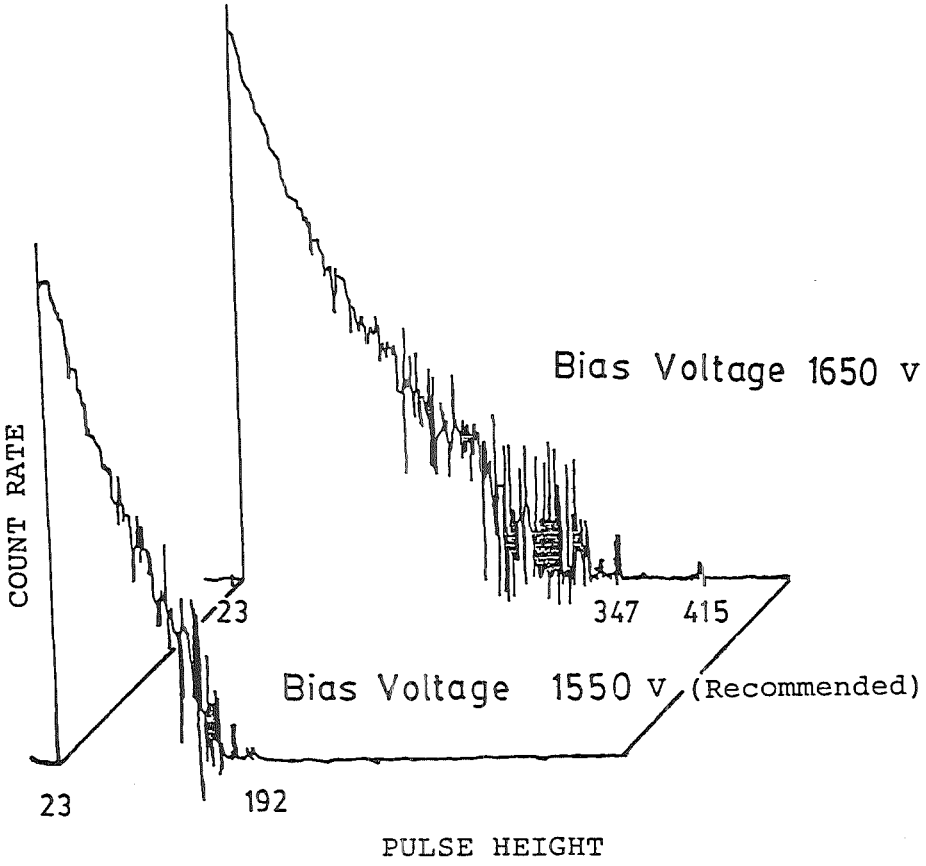

FIG. 22 EXPANSION OF γ -SPECTRUM (4.4mSv/h) OF PROPORTIONAL COUNTER, ^{3}He THOMSON, WITH BIAS VOLTAGE.

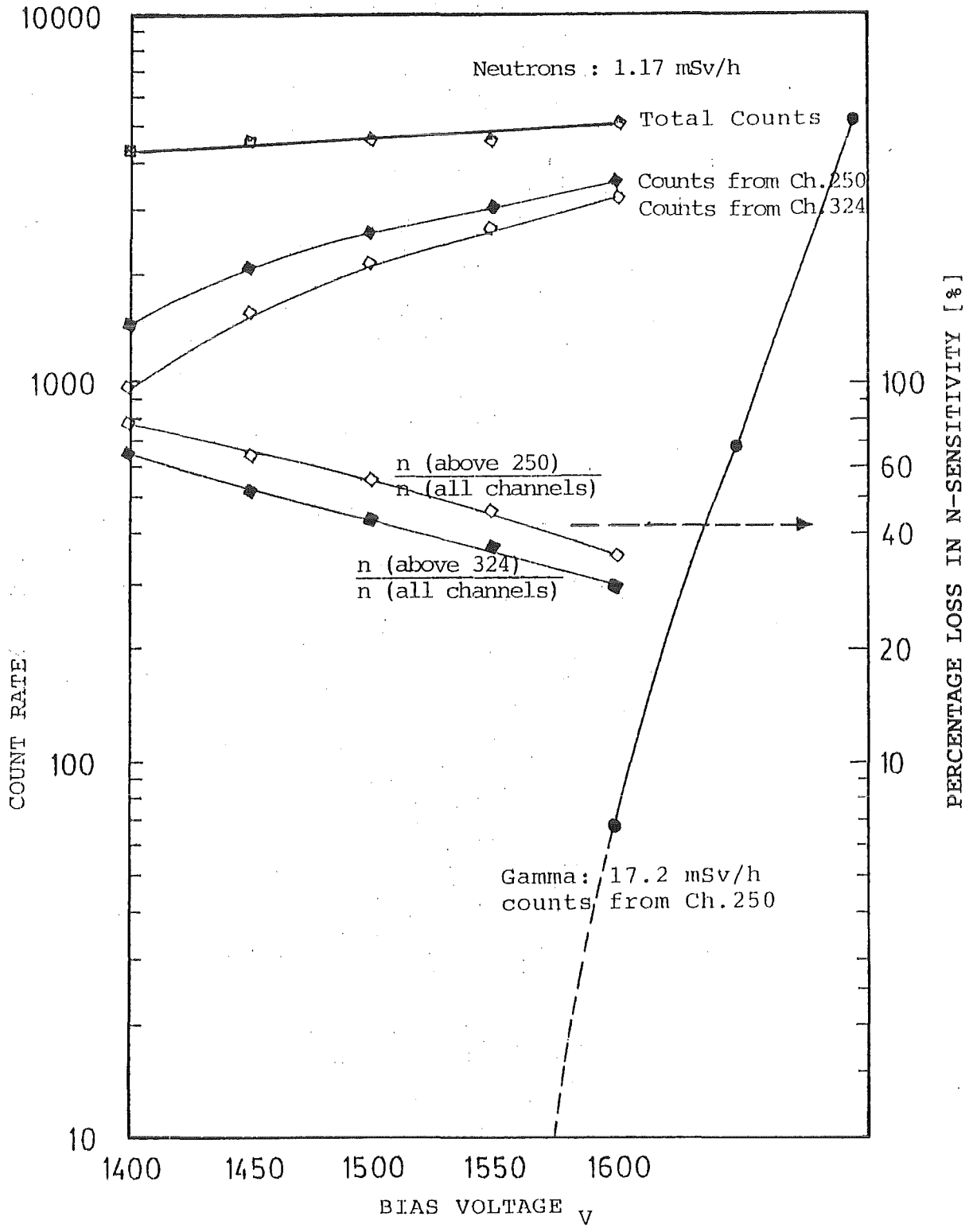

FIG. 23 NEUTRON SENSITIVITY LOSS OF PROPORTIONAL COUNTER, ^{3}He THOMSON, VERSUS BIAS VOLTAGE WHEN COUNTS START FROM CHANNELS 250 & 324.

However, with lower gamma dose rates it is possible to set counts from lower channels [lower than channel 25Ø] by decreasing the pre-amplifier discrimination level. in order to get higher neutron sensistivity if needed, but this will, on the other hand, increase spurious count rates.

The ^{3}He counter showed high neutron sensitivity despite its small volume. It was about twice that of the N.WOOD BF_3 counter and half that of the LND BF_3 counter, when the count of the ^{3}He counter started from channel 25Ø. The reason for the high neutron sensitivity of the ^{3}He counter were its gas pressure which is, about one fold higher than that of the BF_3 counters [section 3] and the higher neutron absorption cross-section of ^{3}He compared with ^{1Ø}B.

Two kinds of pre-amplifiers were used with both kinds of the detectors; Thomson Charge Amplifier ACH and Canberra Model 2ØØ6, which is higher in price. For our purpose, no difference in performance was noticed between the two, therefore, the charge amplifier ACH was chosen. However, it was found that the possible variation in the charge amplifier's discrimination level is limited [this is needed to get good n/γ discrimination at high dose rates]. Therefore a modification was done in the pre-amplifier's electronic circuits which made it possible to raise the discrimination level for the logic signal to the

desired value with a margin. This was achieved using a divider for the incoming signal [2.4 kΩ resistor see figure 24]. A capacitor [1ØØpF] was also inserted to work as a positive feedback to get definite output signals after observing fluctuation in the logic output signals.

The maximum count rates of the ^{3}He detectors are limited by the electronic dead time of the pre-amplifier(*). Dead time measurements were carried out using two neutron sources [Cf 252 and Am/Be] and it was found that the loss in counts is 1% for a count rate of 1ØØØ sec^{-1} [figure 25]. These high count rates rarely faced in actual neutron fields where the system would be used to determine dose equivalent and find calibration factors for personal albedo dosimeters.

It is worth mentioning that some ^{3}He detectors showed significantly different photon and neutron sensitivity. Two detectors out of ten showed double n and γ sensitivities than the others, and one detector showed half the usual sensitivity [see figure 26].

5.2 Central Detector Response Rc

The active part of the ^{3}He detectors used is 1cm long and 1 cm in diameter [≃ Ø.8 cm^{3}], therefore, it is directional

---

(*) Thomson Charge Amplifier ACH, Manufacturer leaflet.

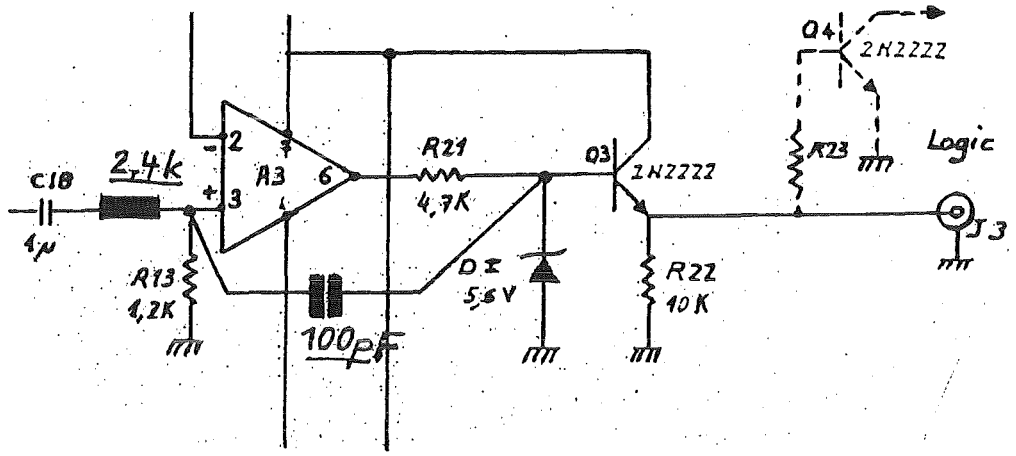

FIG. 24 CHARGES AMPLIFIER ACH SCHEMATIC DIAGRAM, SHOWING THE MODIFICATIONS.

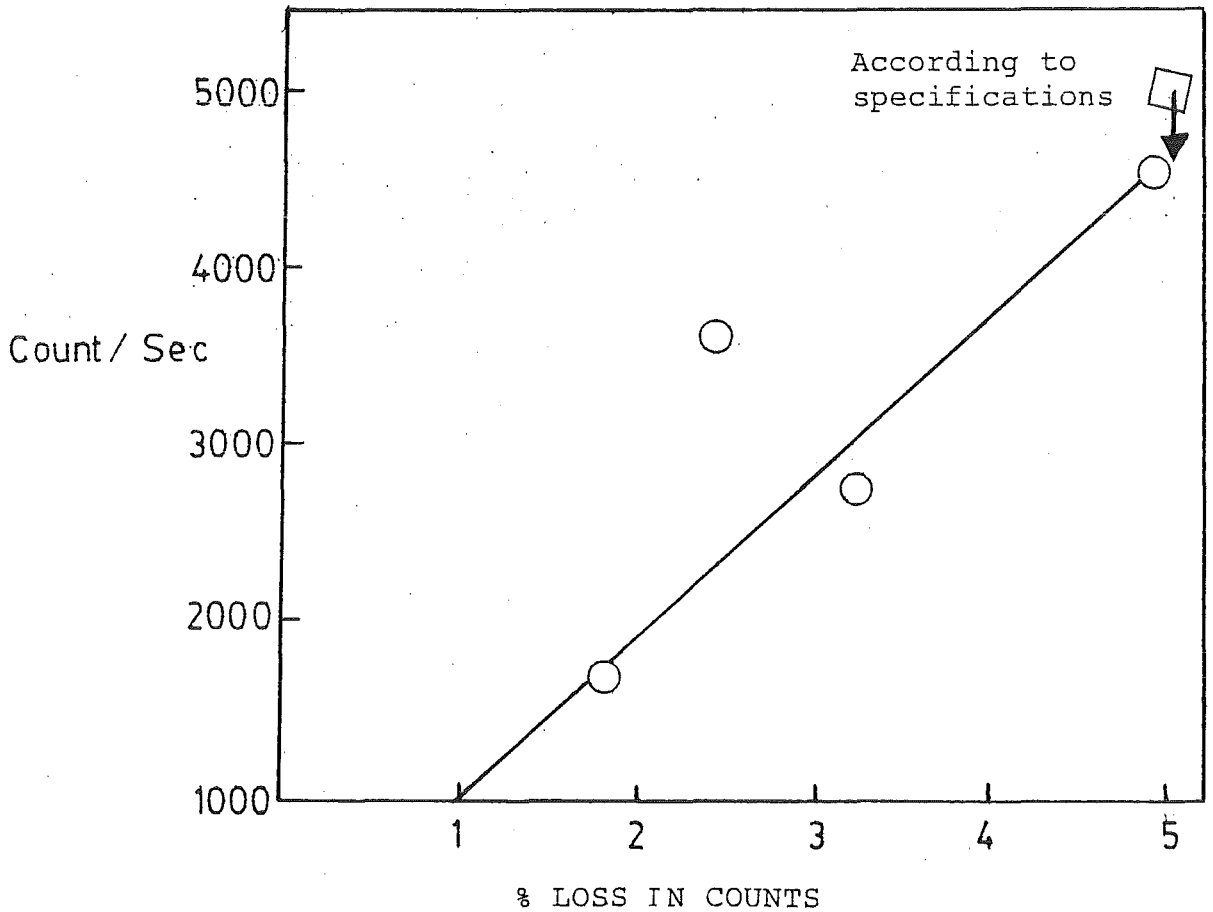

FIG.25 DEAD TIME MEASUREMENT OF ACH PRE-AMPLIFIER USED WITH ^{3}He THOMSON COUNTER.

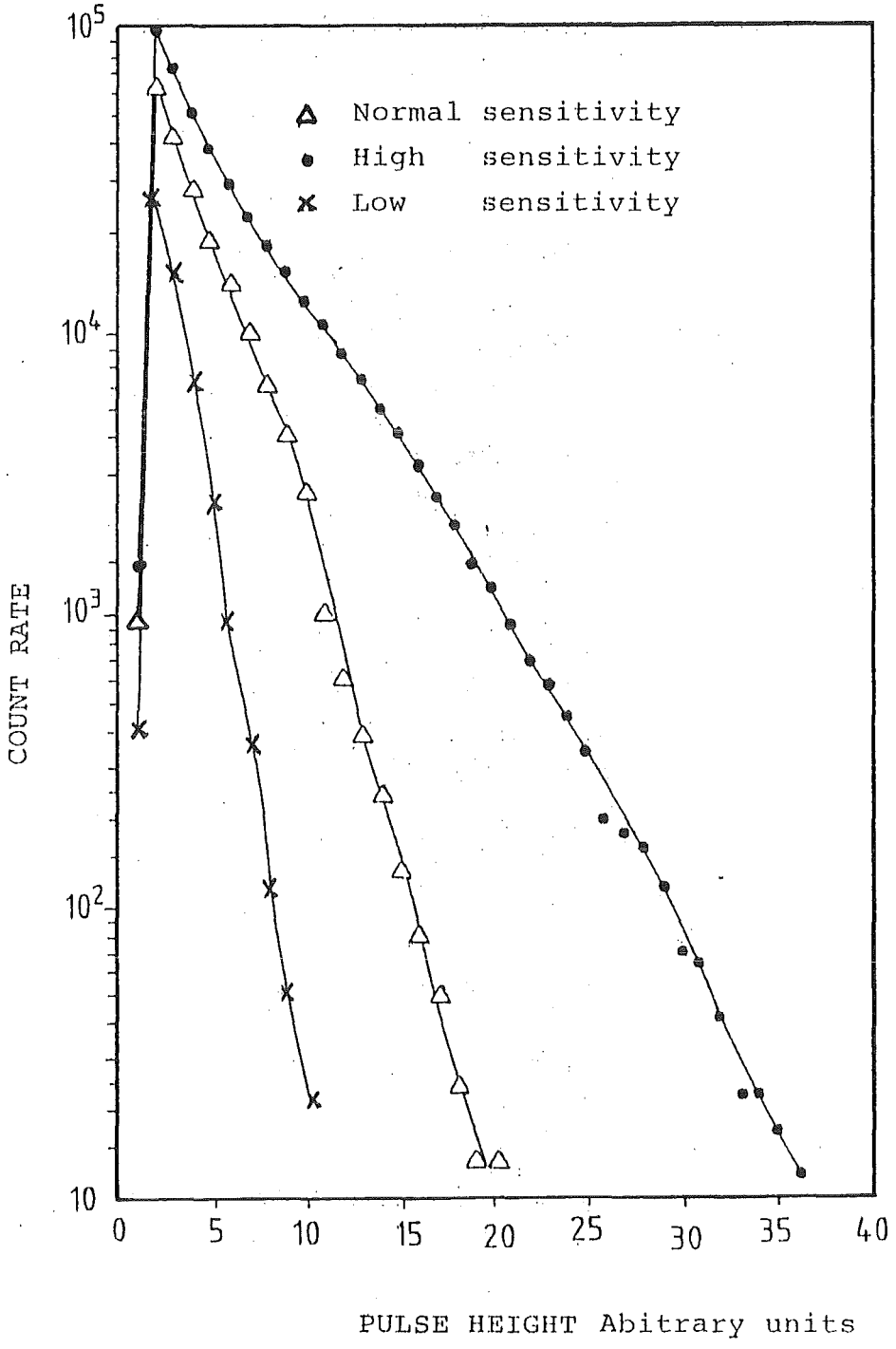

FIG. 26 GAMMA SPECTRA OF THREE PROPORTIONAL COUNTERS, ^{3}He THOMSON, WITH DIFFERENT SENSITIVITIES.

independent in the centre of the PE spheres. Experimental measurements supported this expectation.

Figure 27 shows the experimental values of the response of the central detector in each of the three spheres for different monoenergetic neutrons. The central detector response is given in counts per μSv. The response for the intermediate neutron energy range will be found by calculation. It is apparent for the fast energy range, 10^5 to 1.5×10^7 eV, that the 25cm sphere shows the lowest energy dependence which is $\pm$ 45%.

In previous experiment [11] with BF_3 counters of the studsvik type placed in the middle of 30cm PE sphere similar trend in results was found.

5.3. Albedo Detector Response Ri

The front albedo detector response as a function of detector depth in the PE sphere is shown in figure 28. Figure 28 shows also that Ri response depends, at the same time, on the way in which the detector is inserted in the PE sphere; it is lower when the whole detector is inside the sphere [case (a) in figure 28]. This might be due to absorption of thermal neutrons by the detector wall which is made of Ni and Cu [percentage by weight are 73% and 27% respectively].

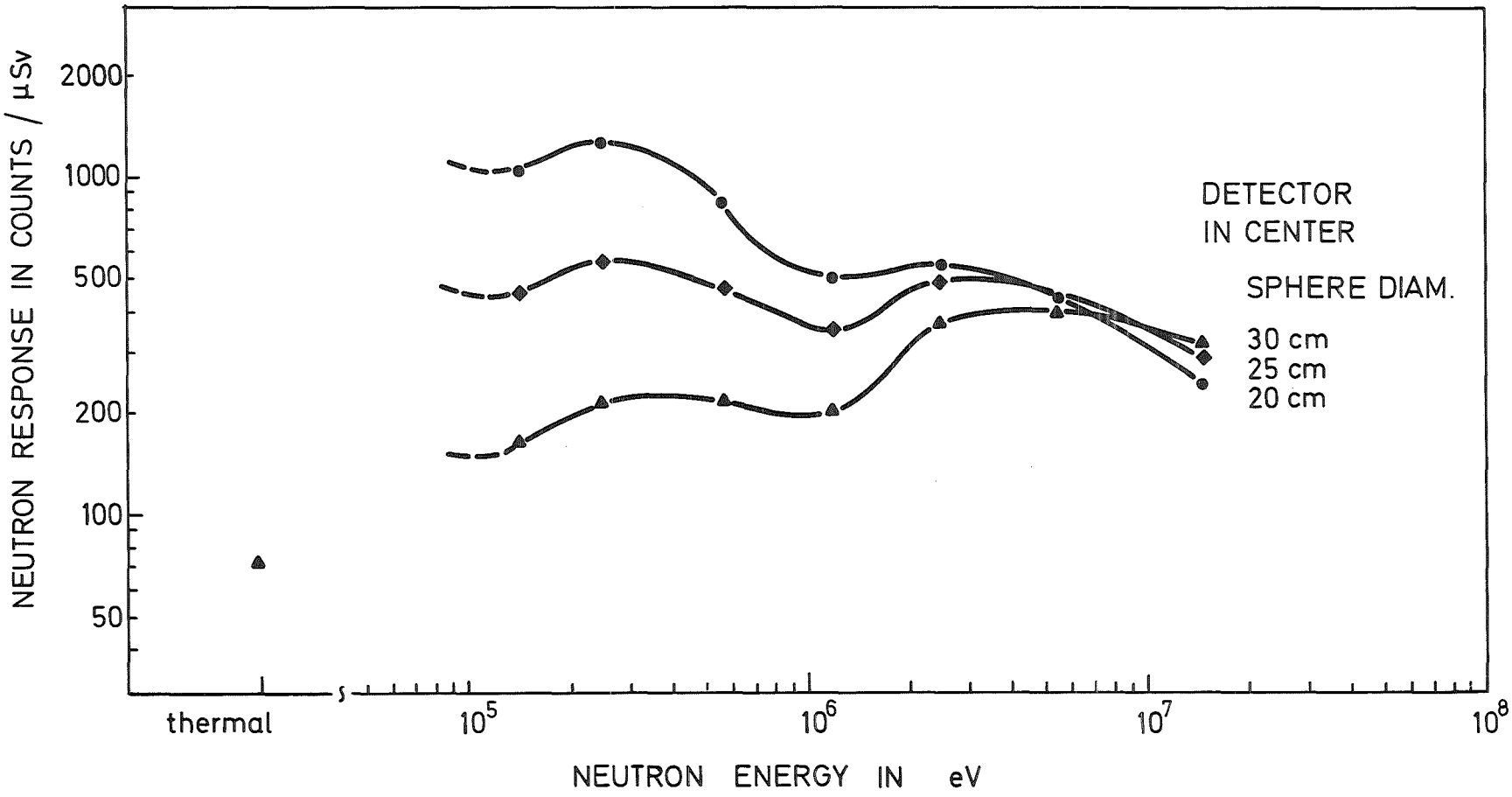

FIG. 27 RESPONSE OF THE CENTRAL DETECTOR TO MONOENERGETIC NEUTRONS

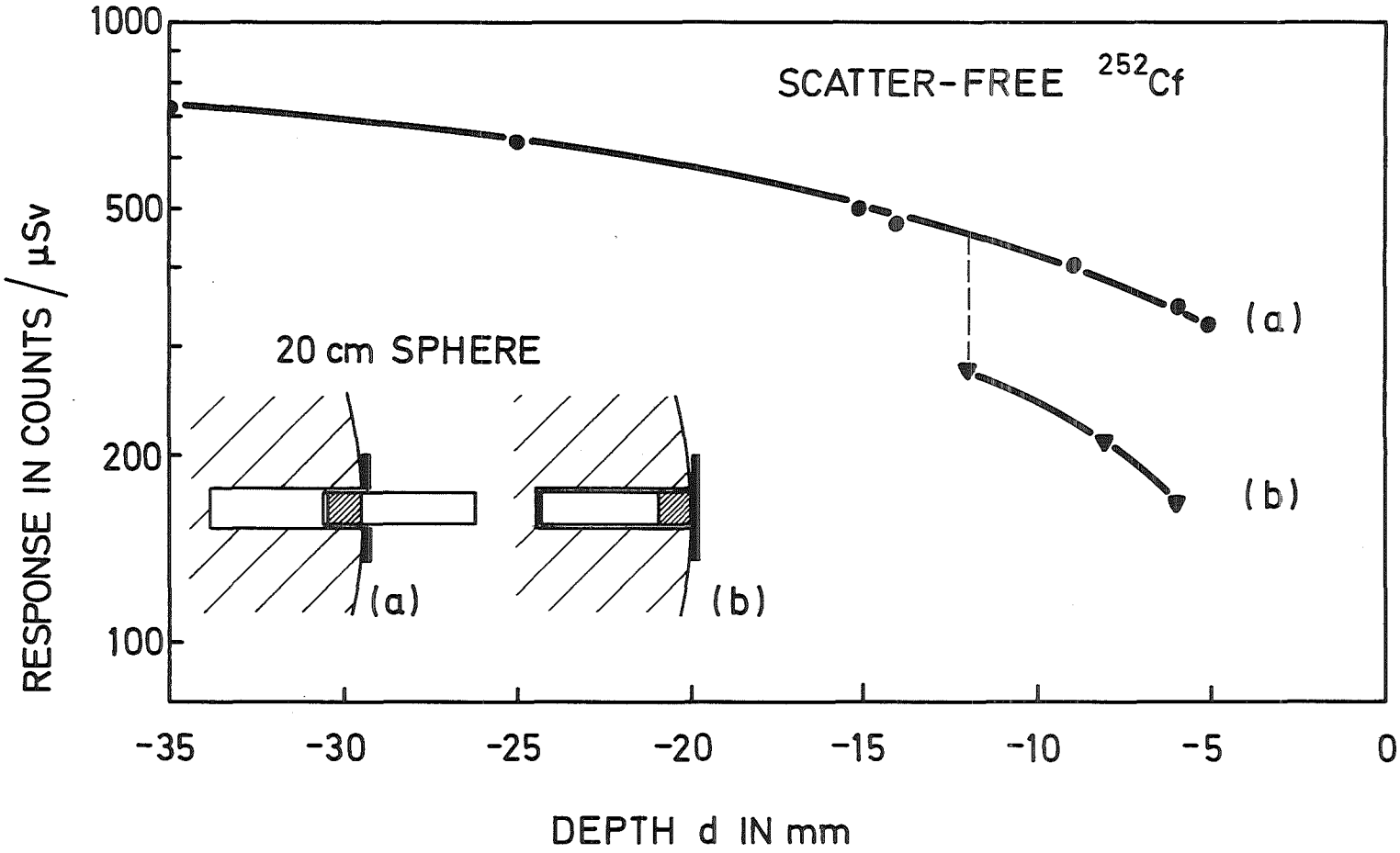

FIG.28 FRONT ALBEDO DETECTOR RESPONSE AS A FUNCTION OF DETECTOR DEPTH IN THE PE SPHERE. (a) WHEN ONLY THE ACTIVE PART OF THE DETECTOR IS INSERTED IN THE SPHERE. (b) WHEN THE WHOLE DETECTOR IS INSIDE THE SPHERE.

5.3.1 Ri response for Cf-252 neutrons

The response of the albedo detector Ri to Cf-252 polyenergetic neutrons versus depth and angle showed similar trend as that of the monoenergetic neutrons as shown in figures 28, 29 and 3Ø.

It was also found that the Ri response for detector depths d < Ø is the same with boron disc and ring [figure 5 shieldings Nos.1 and 2] as expected since the thermal neutron component in Cf-252 neutrons is negligible.

5.3.2 Energy Dependence of Ri

Figure 29 shows the change of the response of the front albedo detector with depth for the different neutron energies. The solid line represent the response of the 2Øcm PE sphere, while the response of the other two sphere is puts as points. It is obvious that the response of the albedo detector decreases with the increase of neutron energy. Moreover, the albedo response as a function of depth follows similar shape in all energies since thermal neuttrons build up for fast neutron beam in the few centimeters depth of polyethyene[4].

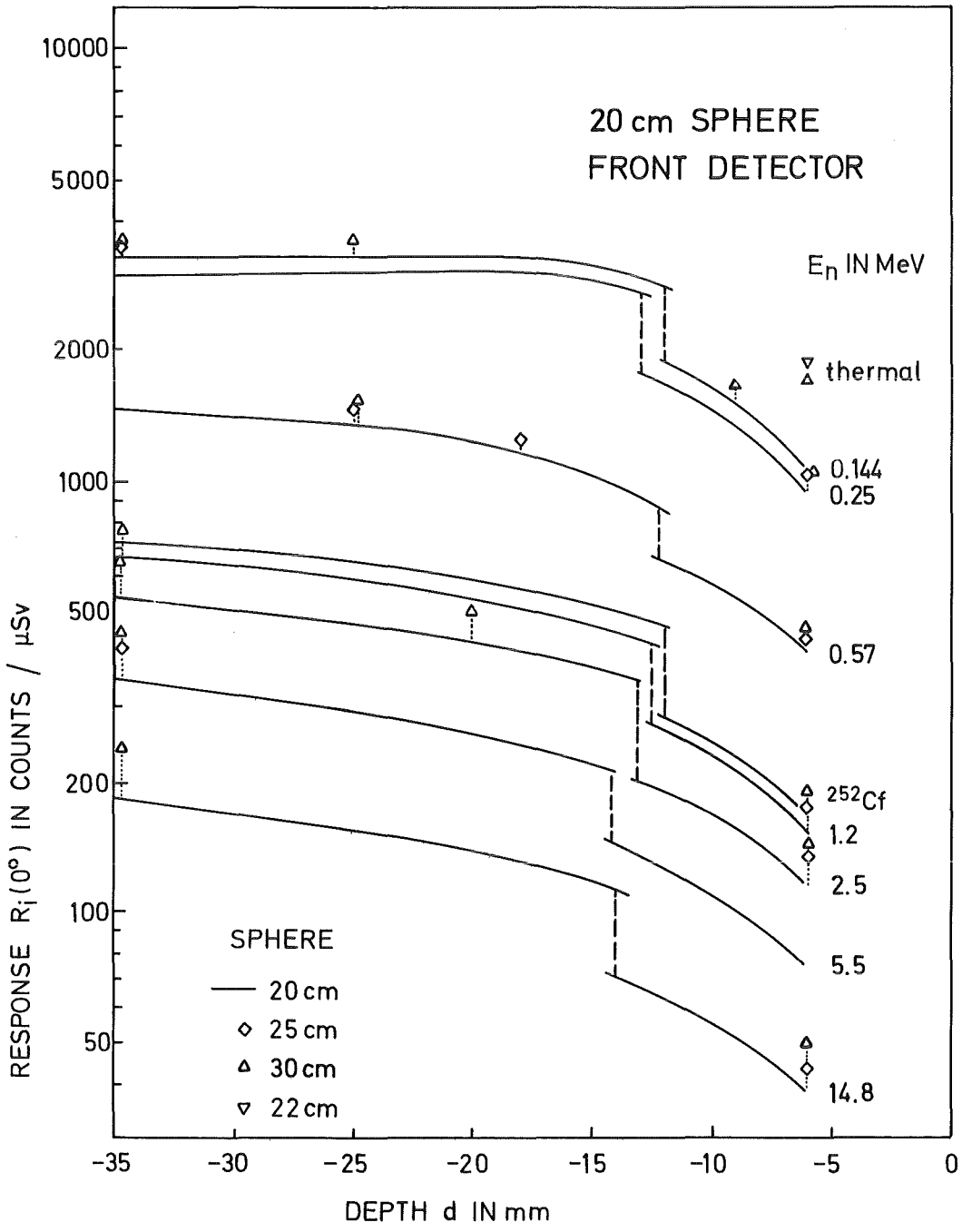

FIG.29 RESPONSE OF THE FRONT ALBEDO DETECTOR AS A FUNCTION OF DETECTOR DEPTH FOR DIFFERENT NEUTRON ENERGIES AND THE THREE SPHERES.

5.3.3 Angular Dependence of Ri

Figure 30 shows the angular variation of the albedo response Ri(∝), for the 2Øcm sphere and a detector depth of d=-6mm. where is the angle of incidence. It is clear that the angular variation increases significantly with the decrease in neutron energy because of the decrease in the neutron penetration power. Figure 31 shows the same response but for detector depth of d=-35mm. The angular variation of the albedo response at this depth is also a function of neutron energy, however, it is less than that for the depth of d=-6mm. In both depths, the ratio of the front Ri(Ø°) to back Ri(18Ø°) responses could be as high as ten for the lower neutron energies like the 25Ø keV and the 144 keV.

Figure 32 shows the angular variation of the sum of two opposite albedo detector readings [Ri(∝)+ Ri(∝ +18Ø°)], normalized to Ri(Ø°), for the depths of d=-6mm and -35mm. The ratio Ri(∝)+ Ri(∝ +18Ø°)/ Ri(Ø°) for all angle of incidence increases with the increase of neutron energy due to the increase in neutron penetration power. This is an advantage if two albedos detectors going to be used at two opposite directions because this will minimize the difference in the absolute albedo detector response [counts/ μSv] with the neutron energy, which was found to increase with the decrease of neutron energy [see figure 28].

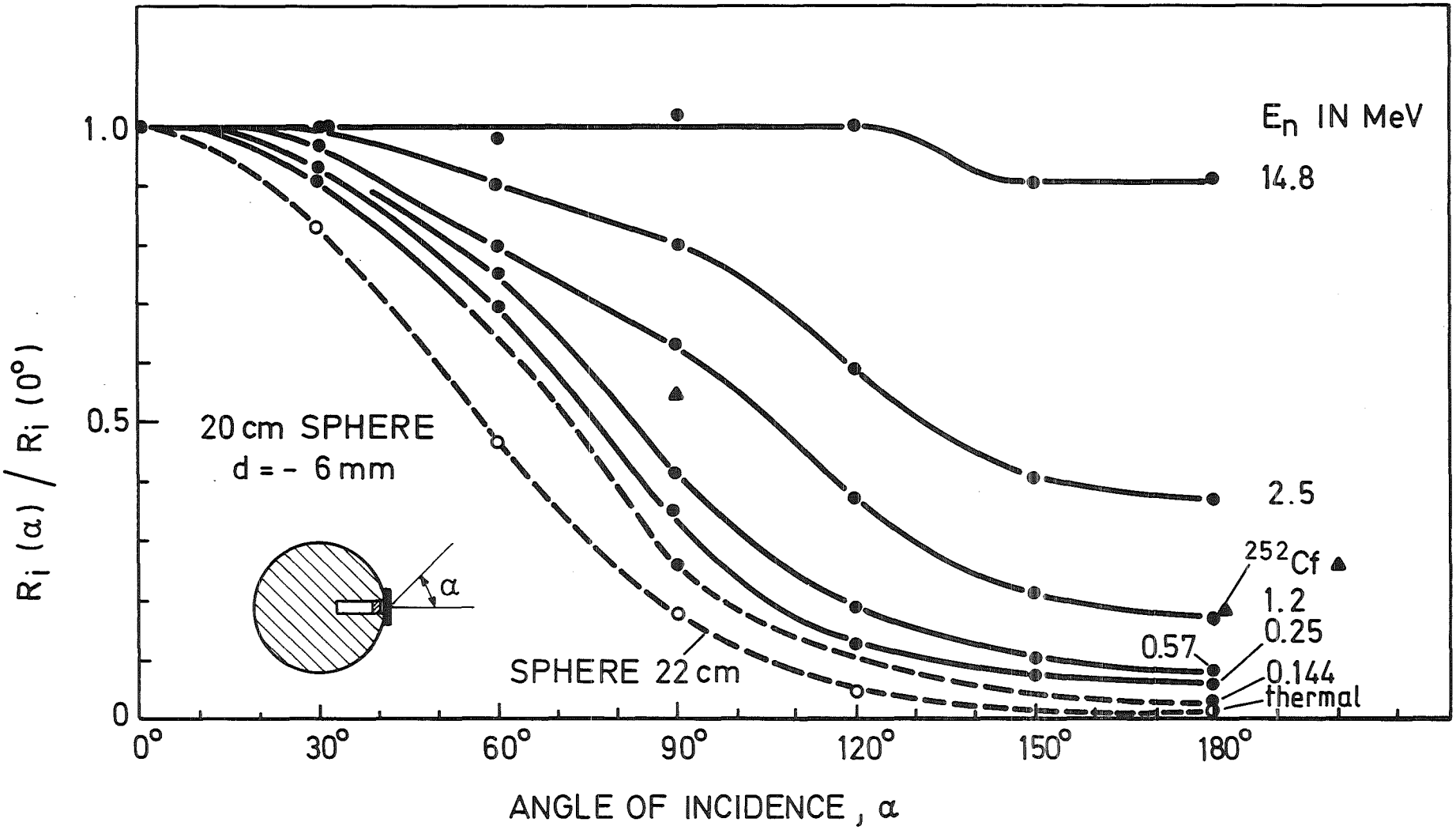

FIG.30 RESPONSE OF THE ALBEDO DETECTOR READING, NORMALIZED TO THE FRONT, VERSUS ANGLE OF INCIDENCE FOR THE 20cm SPHERE AND A DETECTOR DEPTH OF -6mm.

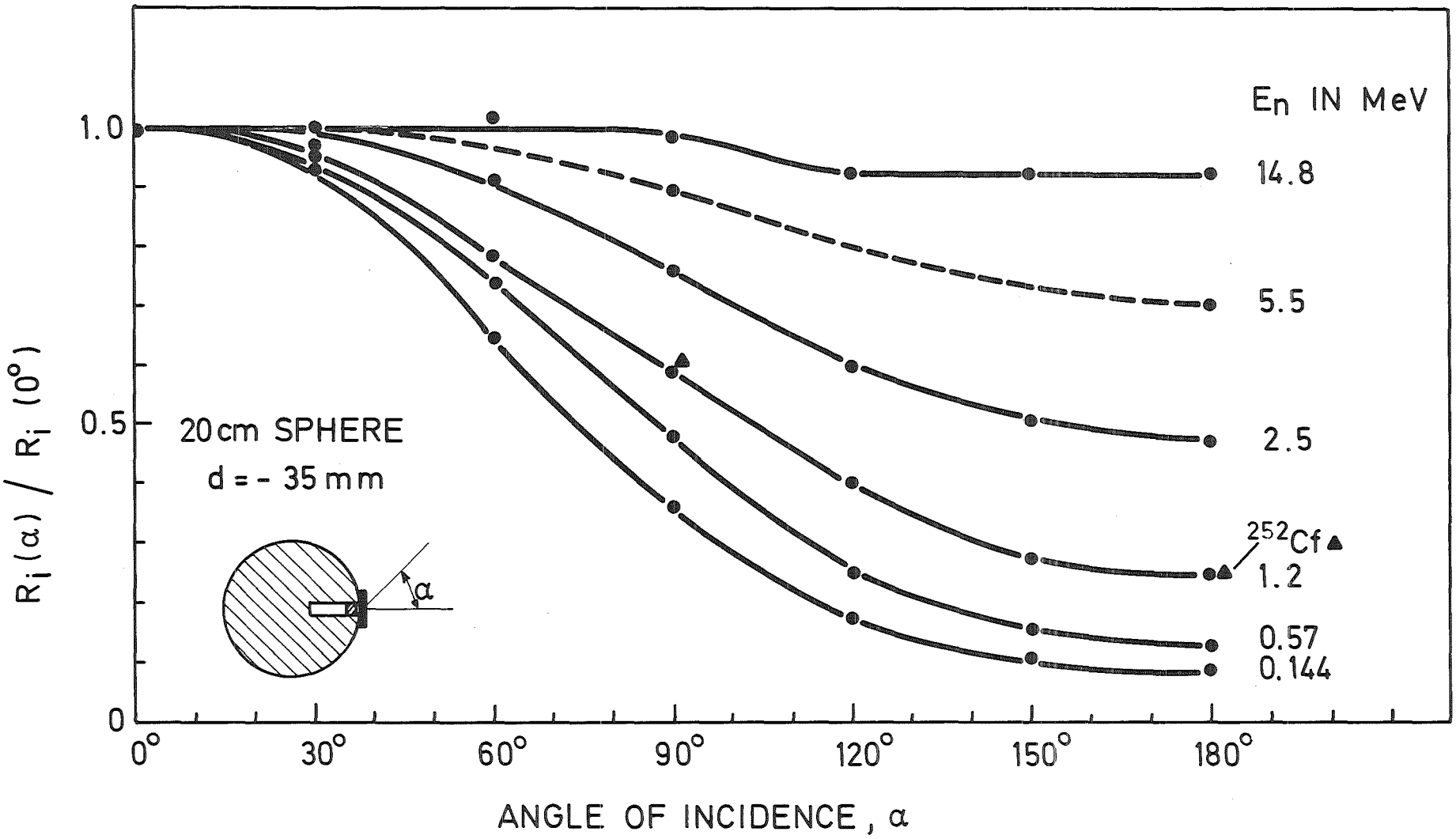

FIG.31 RESPONSE OF THE ALBEDO DETECTOR READING, NORMALIZED TO THE FRONT, VERSUS ANGLE OF INCIDENCE FOR THE 20cm SPHERE AND A DETECTOR DEPTH OF -35mm.

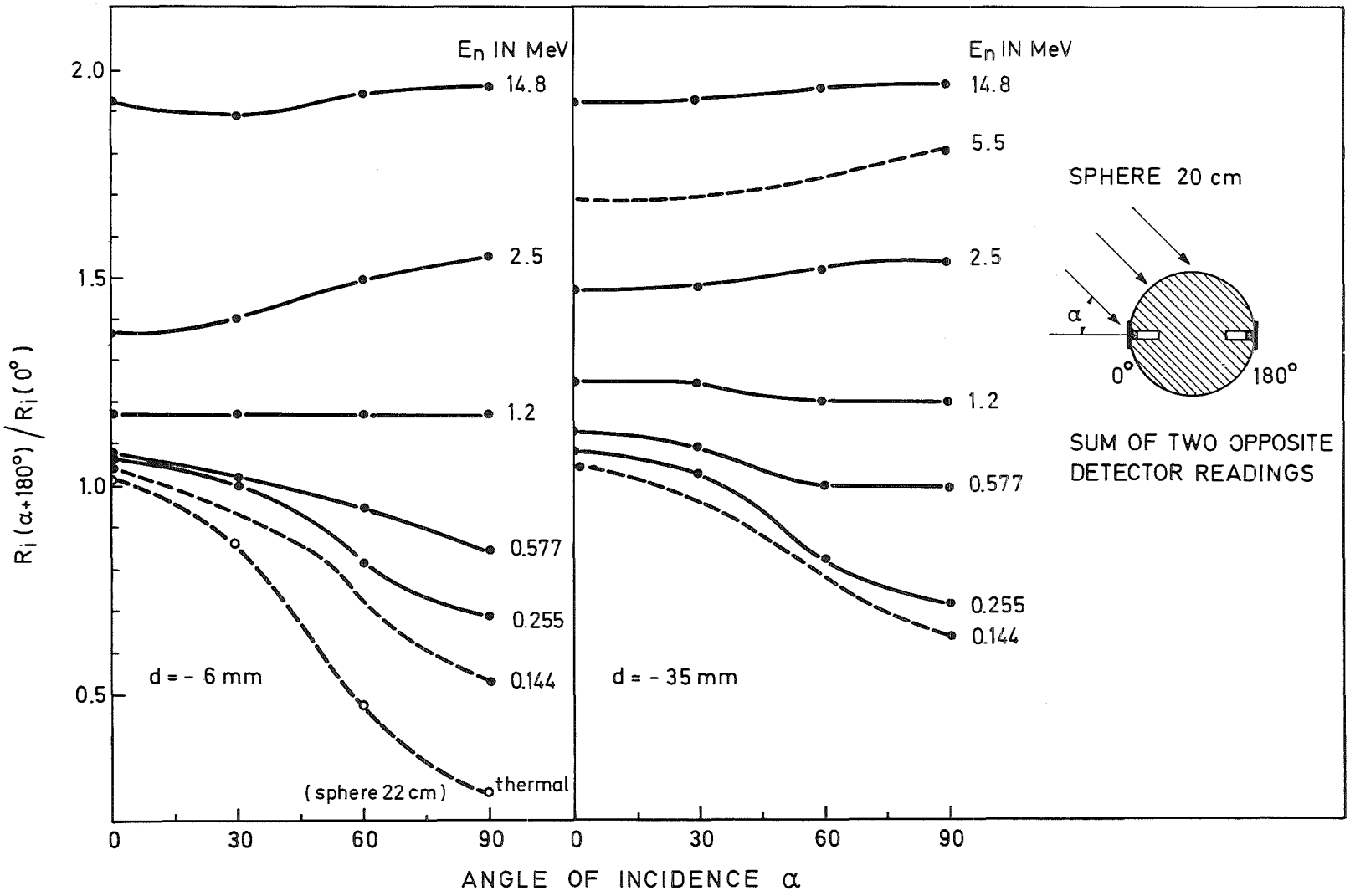

FIG.32 RESPONSE OF THE SUM OF TWO OPPOSITE ALBEDO DETECTOR READING, NORMALIZED TO THE FRONT ALBEDO READING, VERSUS ANGLE OF INCIDENCE FOR THE 20cm SPHERE AND DETECTOR DEPTHS OF -6mm AND -35mm.

Figure 33 shows the albedo response ratio Ri(rotation)/Ri(Ø°) versus neutron energy for the three spheres and the two detector's depths. The Ri(rotation) was found by adding Ri(Ø°)+Ri(9Ø°)+Ri(18Ø°)+Ri(27Ø°) and then dividing the sum by four. By comparing this figure with figure 30 or 31 , it is clear that the rotation reduces the angular variation of the albedo response by about a factor of four at the lower neutron energies where the angular dependece is high. It is also obvious that the ratio Ri (rotation)/Ri(Ø°) increases with the increase in neutron energy due to the increase in neutron penetration power as mentioned earlier.

5.3.4 Variation of Ri response with sphere size

Figure 34 shows the variation of the absolute albedo response [front, α =Ø°] with neutron energy for the three spheres at the detectors depth of -6mm. It is clear that the albedo response increases slightly with the increase in sphere size. However, it was found that the albedo response is significantly higher for depth d=-35 than for depth d=-6mm by more than four fold.

Figures 35 & 36 show the variation of the albedo response ratio Ri(α)/Ri(Ø°) with the angle of incidence α for the three spheres and the detector depths of -6mm and -35mm respectively.

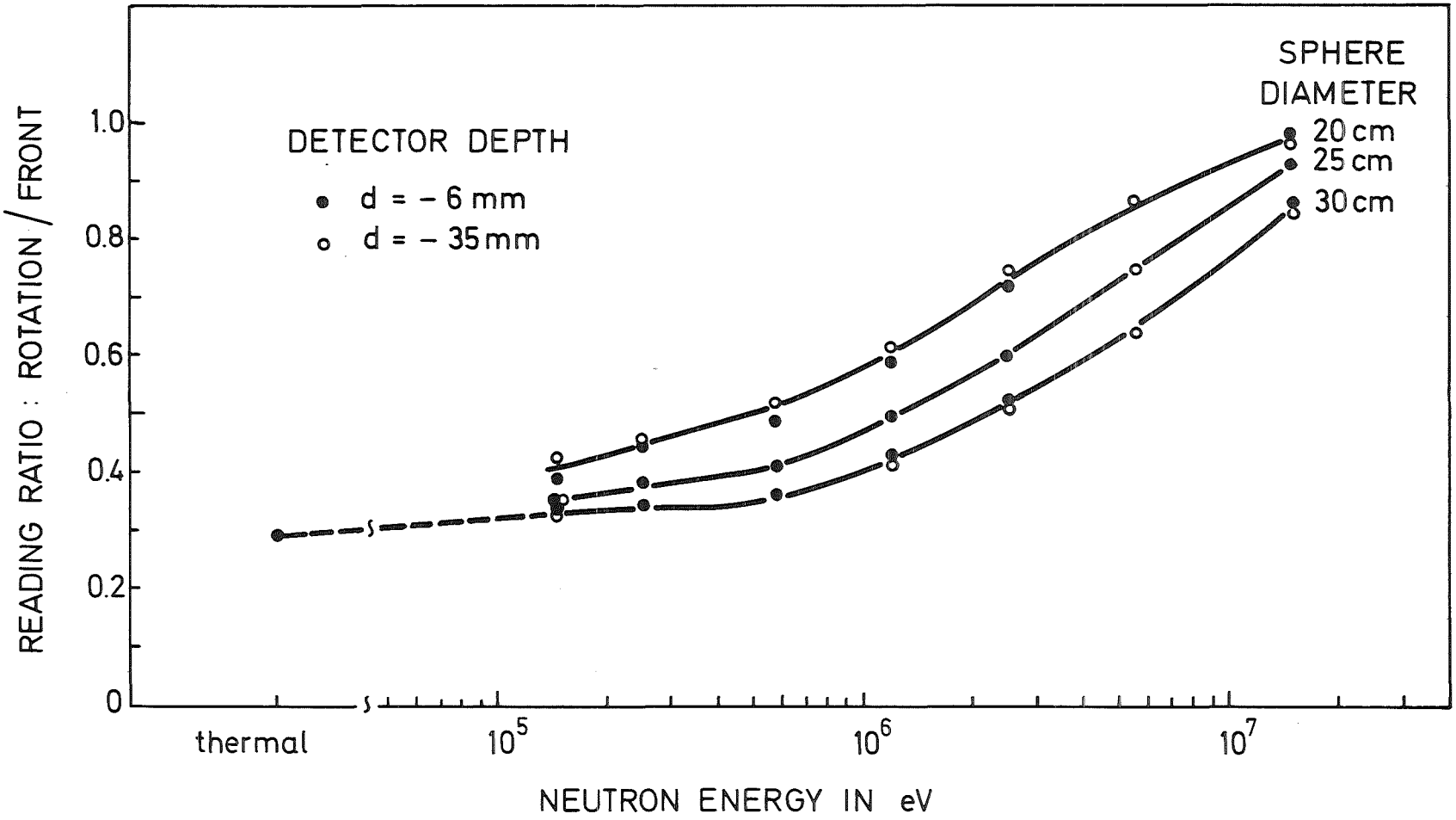

FIG.33 RESPONSE OF THE ROTATING ALBEDO DETECTOR READING, NORMALIZED TO THE FRONT, VERSUS NEUTRON ENERGY FOR THE THREE SPHERES AND THE DETECTOS OF -6mm AND -35mm.

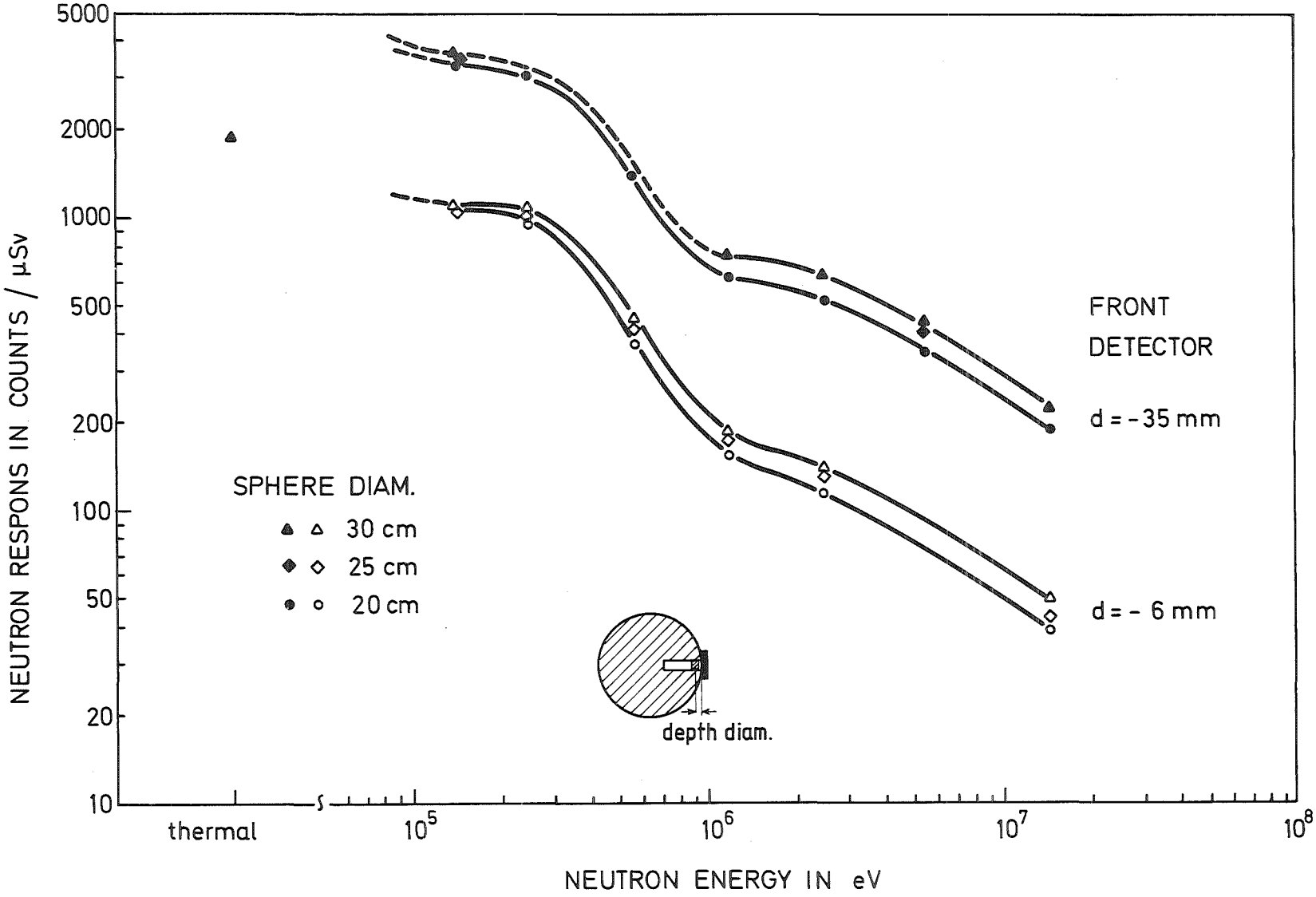

FIG.34 RESPONSE OF THE FRONT ALBEDO DETECTOR VERSUS NEUTRON ENERGY FOR THE THREE SPHERES AND THE TWO DETECTOR DEPTHS OF -6mm AND -35mm.

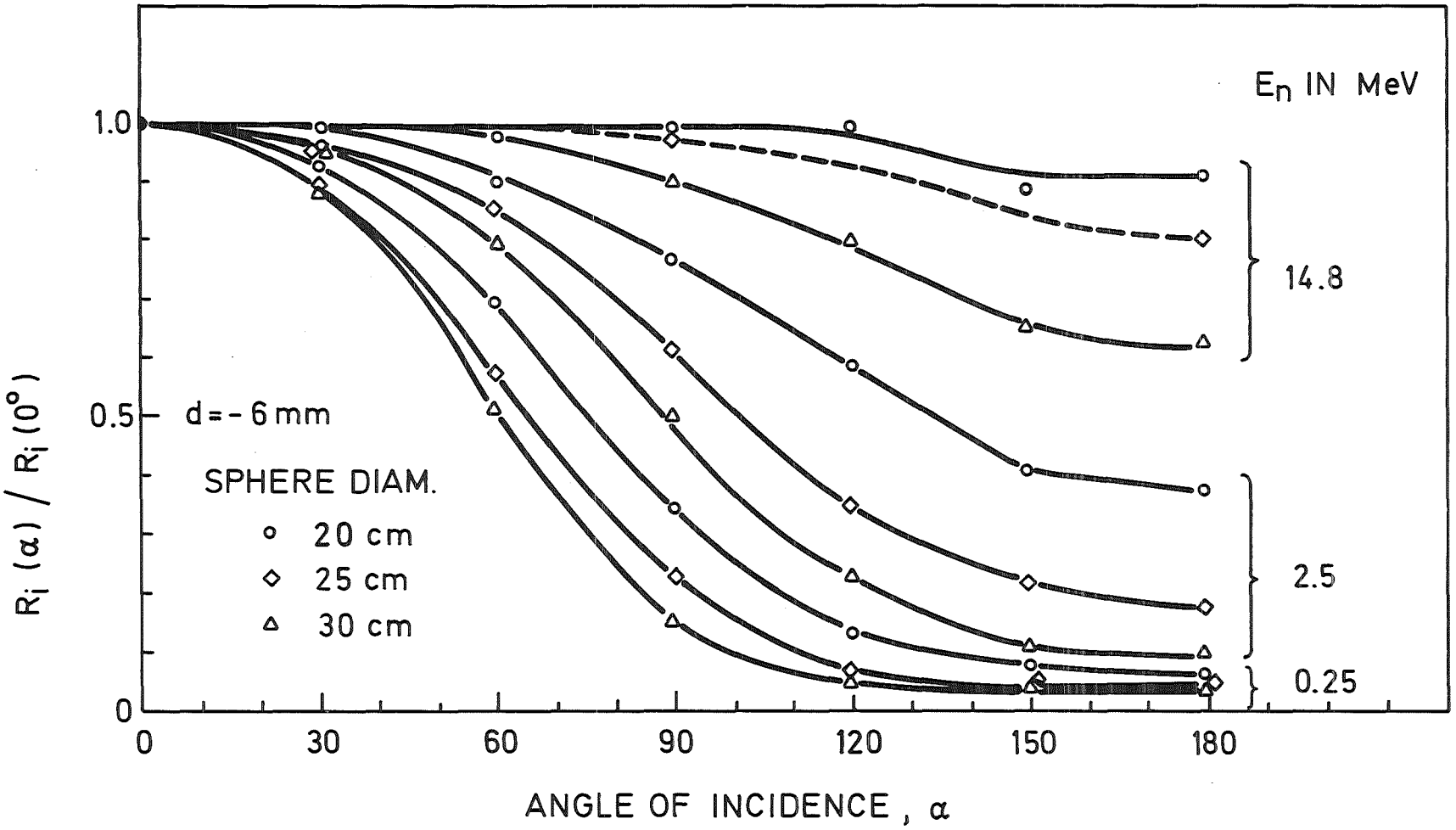

FIG.35 RESPONSE OF THE ALBEDO DETECTOR READING, NORMALIZED TO THE FRONT, VERSUS ANGLE OF INCIDENCE FOR THE THREE SPHERES AND A DETECTOR DEPTH OF -6mm FOR NEUTRON ENERGIES 14.8, 2.5 AND 0.25 MeV.

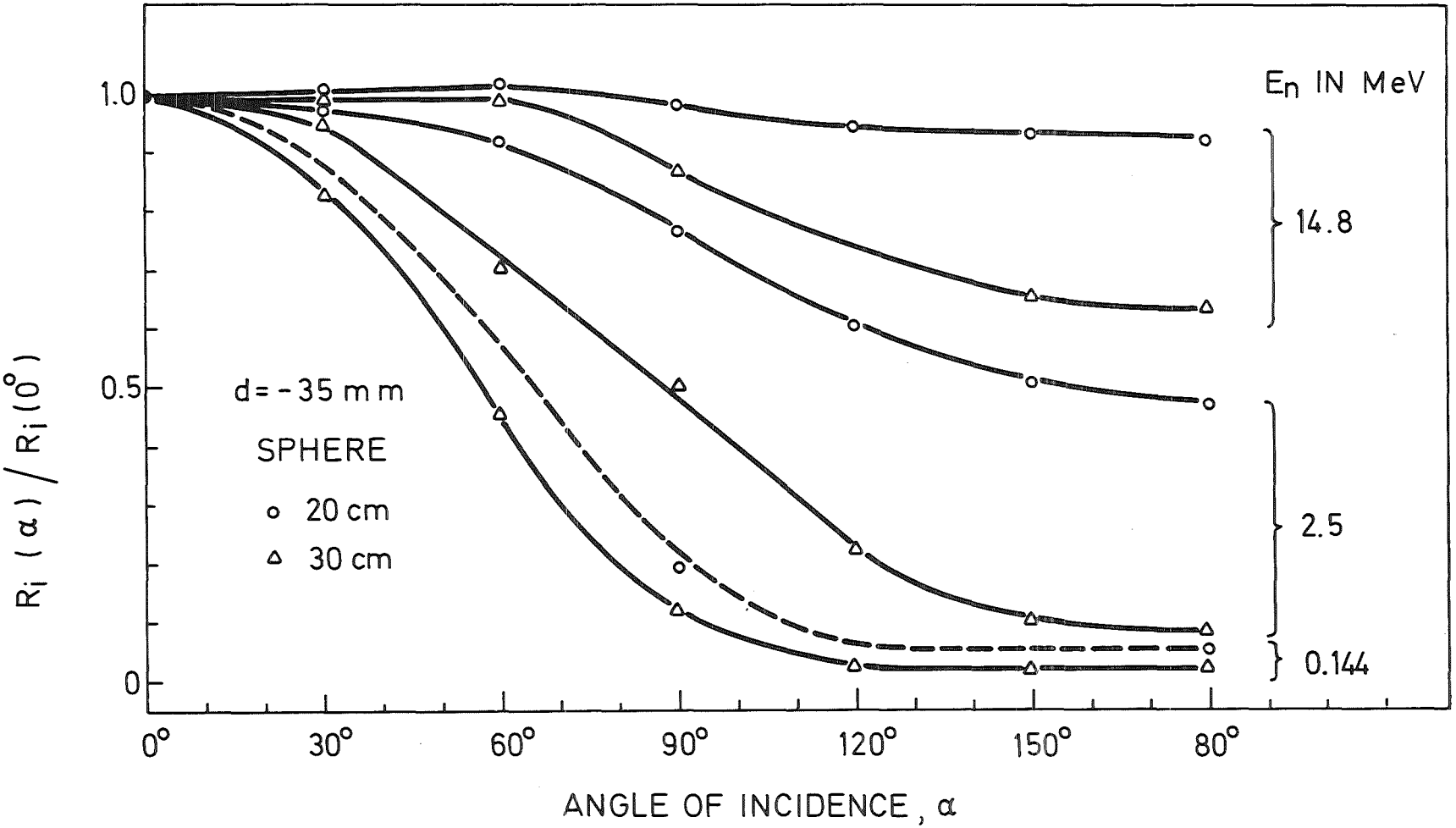

FIG.36 RESPONSE OF THE ALBEDO DETECTOR READING, NORMALIZED TO THE FRONT, VERSUS ANGLE OF INCIDENCE FOR THE THREE SPHERES AND A DETECTOR DEPTH OF -35mm FOR NEUTRON ENERGIES 14.8, 2.5 AND 0.144 MeV.

It is apparent in both graphs that the ratio Ri(α)/Ri($\emptyset^{o}$) values for the depth d=-35mm is slightly higher than that of depth d=-6mm and this was seen previously in figures 30 and 31. It is also apparent from these two figures that the angular variation of the albedo response increases with the decrease in neutron energy and with the increase in the sphere size.

5.4 Thermal Detector Response Ra

The thermal detector is used to measure mainly the direct thermal neutrons which are coming from the radiation field [section 1]. With monoenergetic fast neutron beam there is no thermal neutron component. However figure 37 shows a thermal neutron component [given in absolute values: counts/μSv]. This could come from two sources; first, back scattered neutrons from the surrounding which are thermalized in the scattering process. This is supported by the readings of a detector located in a position close to the PE sphere, and represented by the FREE IN AIR values in figure 35. The other contribution of thermal neutrons could come from back scattered neutrons from the polythylene [C and H] sphere itself. In the case of shielding No. 4 in figure 5, a boron tube surrounding the ^{3}He counter is used for the absorption of the thermal neutron component, however, in shielding No.6 the boron tube plus the boron cup is

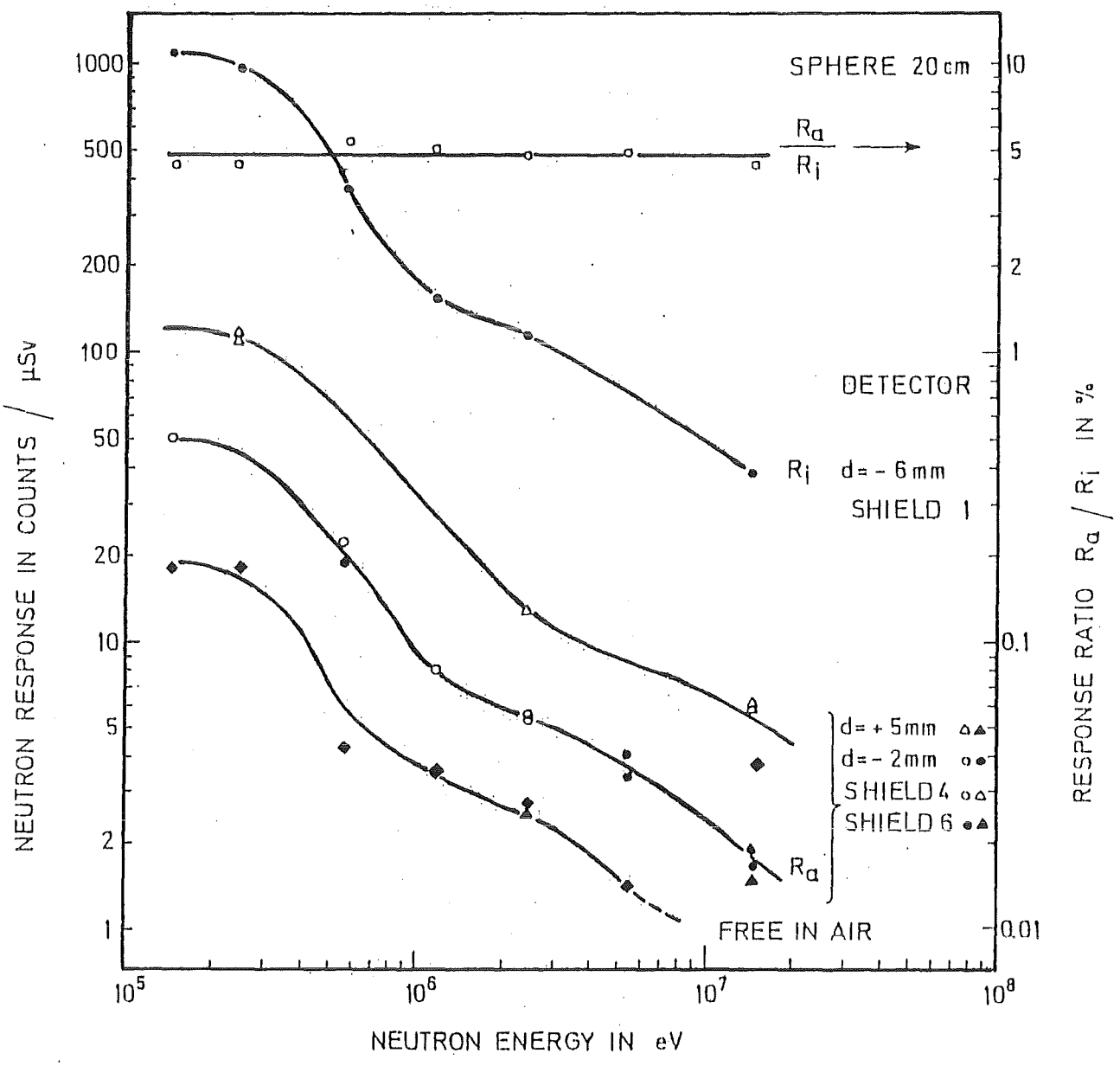

FIG. 37 THERMAL DETECTOR RESPONSE VERSUS NEUTRON ENERGY FOR THE 20CM PE SPHERE. THERMAL TO ALBEDO RESPONSE IS DRAWN ALSO.

used as shown in figure 5, to eliminate back scattered neutrons coming from the surrounding. Therefore, the thermal neutron component in the first case [shielding 4 in figure 5] is higher than in the case of shielding No.6. In all cases, the uncertaintity in the thermal neutron components is higher than that of the albedo and the central detector measurements because of low counts [statistical errors < 7%].

Figure 37 shows that the Ra response increases with the decrease in neutron energy, since less number of collisions are required to thermalized neutrons with the decrease in neutron energy. The ratio Ra(shilding 6)/Ri is also drawn in figure 37 which shows that this ratio is constant and equal to about Ø.Ø5 or 5% only.

The thermal neutron response drawn in figure 37 is for the 2Øcm PE sphere, and the response for the other spheres is similar.

5.5 Estimation of the uncertainty in the Measurements

Measurement's uncertainties are mainly statistical. This statistical uncertainties in counts are very small due to the high total counts taken as is apparent from [Appendix 1]. However, for Ra measurements [FIG.37 only] in fast neutron fields, the statistical uncertainty in individual reading could

be, some times, as high as 7% for the front detector. These uncertainties are covered in the figure by the drawn point sizes, therefore, there are no need to draw error bars.

Using passive detectors [section 6], the percentage uncertainties are written in Appendix 2 and are usually below 2.5%.

6. Comparison Between Active and Passive Measurements

Active and passive neutron measurements were carried out in the stray neutron fields at DKFZ [section 4.4] with single sphere albedo technique. The measurements were done to find out the correlation of the albedo response normalized to the reference value of the dose equivalent [Ri/Rc] with reading ratio Ra/Ri, and to make a comparison between active and passive detectors.

Figure 38 shows the correlation between the Ri/Rc ratio [where Rc represent dose equivalent measurement] with the ratio Ra/Ri for the two PE spheres; 30cm and 20cm diameter. It is apparent that the two readings are correlated [i.e. fits a straight line]. The same figure 36 shows the correlation between [Ri(0°)+Ri(180°)]/Rc with the reading ratio [Ra(0°)+Ra(180°)]/[Ri(0°)+Ri(180°)], which shows that including back detectors readings; [Ra(180°)] and [Ri(180°)], did not improve the correlation. This correlation is important to estimate actual calibration factors of albedo dosemeter in neutron routine monitoring to correct for energy dependence [see section 2]. More measurements are required with the active system after the final optimization of the system to cover more locations in DKFZ hall and establish the correlation.

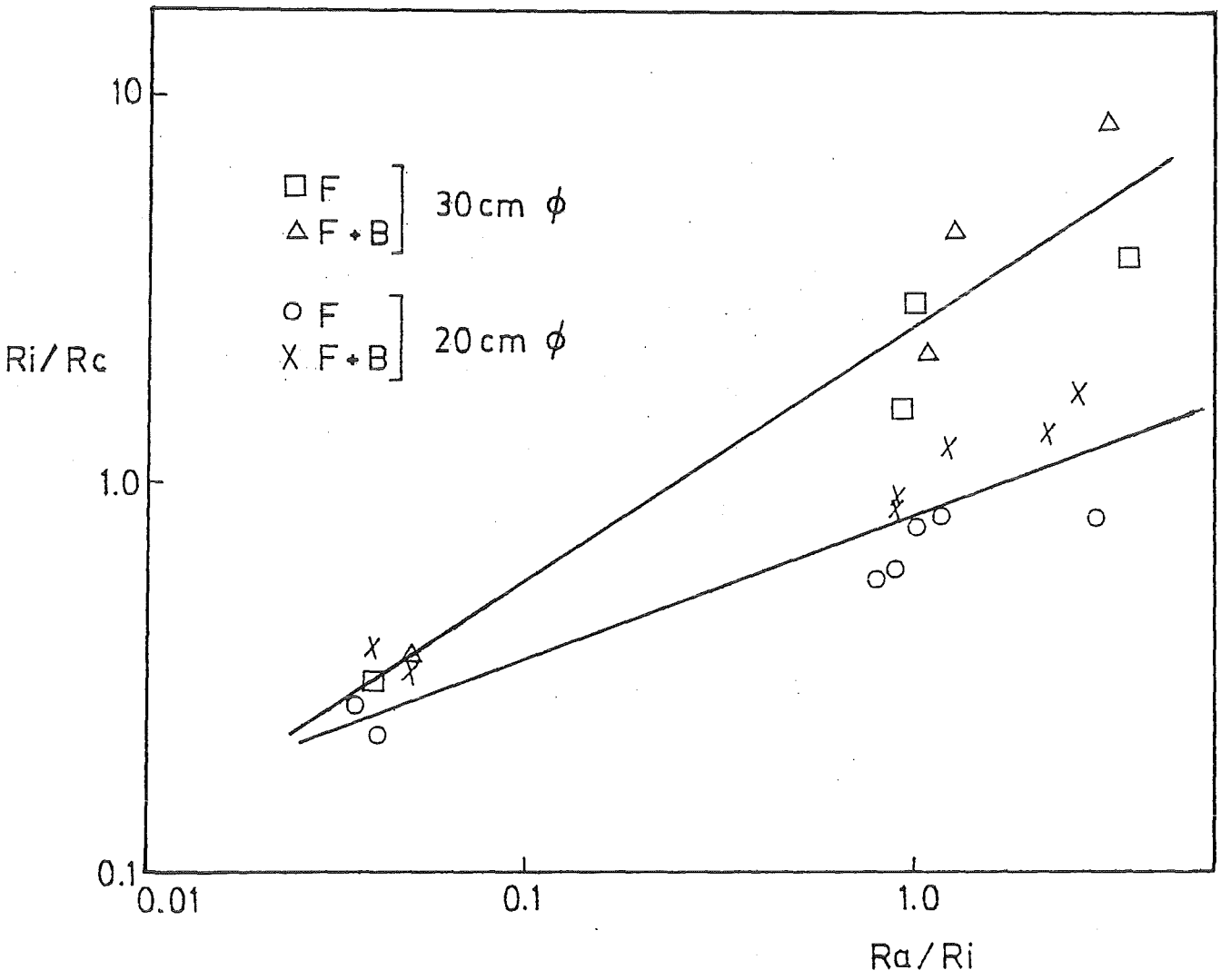

FIG.38 : R_i/R_c VERSUS R_a/R_i FOR ACTIVE ALBEDO SYSTEM WITH PE SPHERES 30cm AND 20cm.

Figure 39 shows the correlation between Ri/Rc and Ra/Ri for the passive detector system for the measurements carried out in the same DKFZ hall. The data could be approximated to a straight line.

The Ra/Ri ratio for active and passive systems were found correlated except at the point in line with the neutron beam and very near to the target (see figure 40).

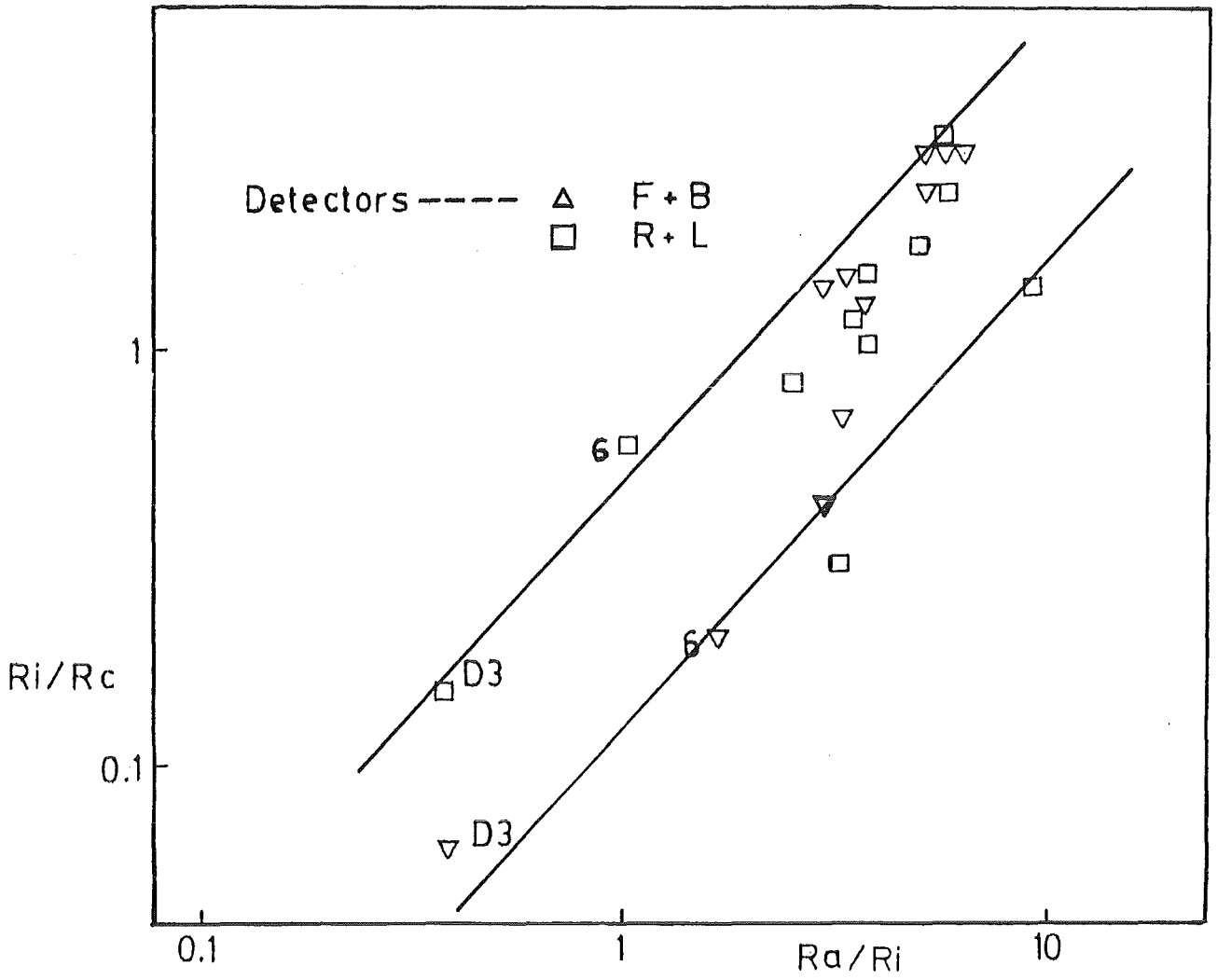

FIG.39 R_i/R_c VERSUS R_a/R_i FOR PASSIVE ALBEDO SYSTEM

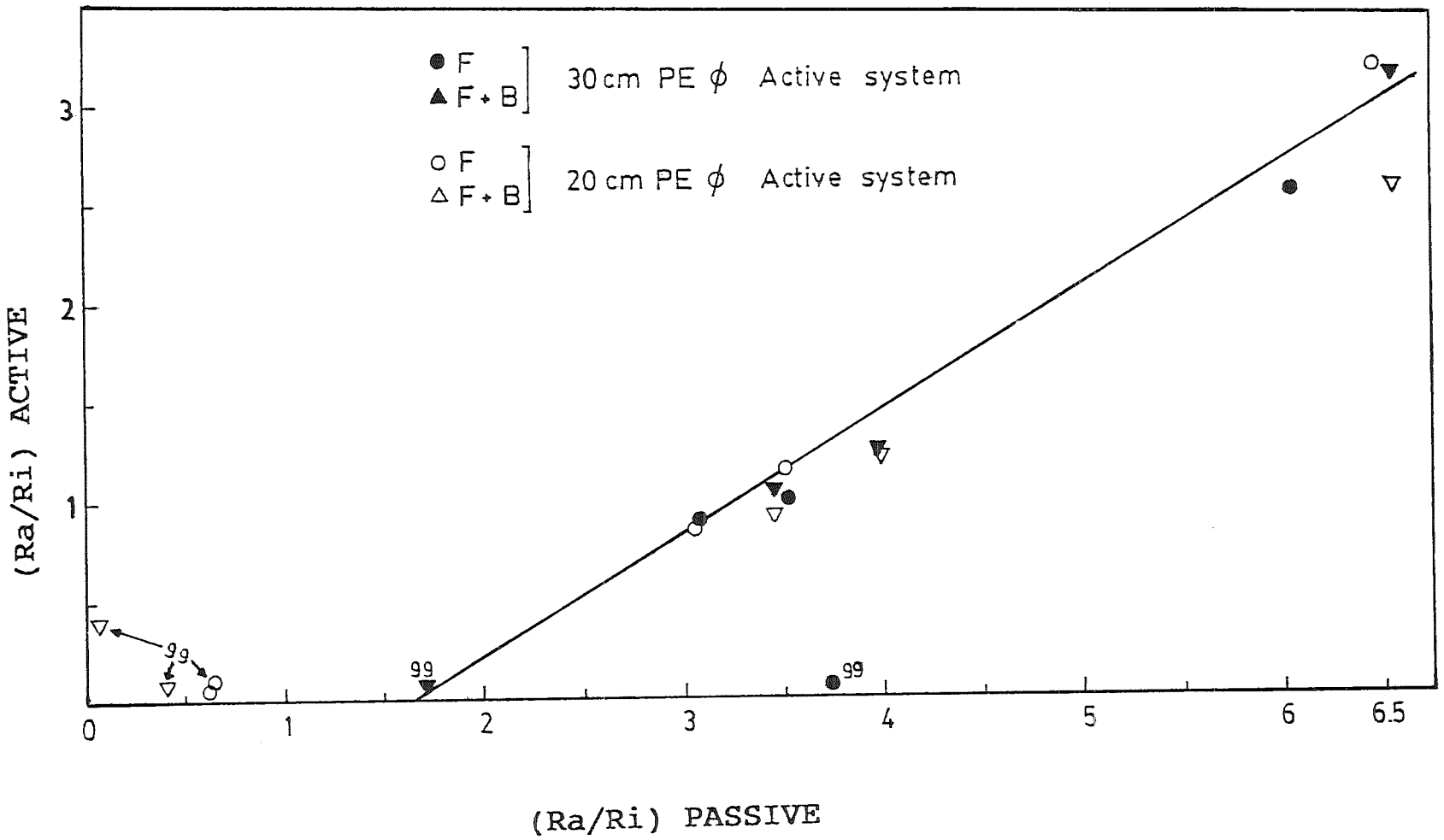

FIG.40 R_a/R_i RATIO OF SSA ACTIVE DETECTORS VERSUS R_a/R_i RATIO OF SSA PASSIVE DETECTORS USING THE 30 Cm PE SPHERE IN STRY NEUTRON FIELDS.

7. Final Optimization of the System

To optimize the system one have to consider the different factors effecting Rc, Ri and Ra to choose the optimium conditions. These factors include detector depth of albedo and thermal detectors, absorber shape, sphere size and whether to have a rotating system or not.

For the depth of the albedo detector (i) it was found that increasing detector depth from -6mm to -35mm increases detector response by at least, two fold as shown in fig.34 for monoenergetic neutrons and for Cf-252 neutrons. However the increase in Ri response is not necessary because the ratios Ri/Ra and Ri/Rc are already higher by a factor of 3.6 compared with the passive single sphere. Moreover, with depth -6mm, the wire - detector connection is hidden in the PE sphere and safe from damage. Therefore, for the detector (i) a depth of -6mm was chosen.

The boron shielding ring (fig.5 No.2) used with the detector (i) was found sufficient to eliminate thermal neutron components in fast neutron fields [Cf-252]. However, in neutron field with a high thermal neutron component it is necessary to use a boron cup [fig.5 No.3] or it is even better to use a single boron disc (figure 5 No.1) to eliminate direct thermal neutrons from being detected by the albedo detector (i).

For the thermal neutron detector (a) it would be better to have all the active part of the ^{3}He detector showing outside the PE sphere [i.e. d $\geq$+5mm, see fig.5 No.4]. This will increase the sensitivity of the detector [see fig.37]. The ratio of Ra (shielding No.4, d=+5mm) and Ri (shielding No.6, d=-6mm) agree best with the passive system. However, having the detector outside the PE sphere will expose it to damage, therefore, a detector protection cover ,made from a suitable material and thickness, could be used by fixing it to the PE sphere.

The shielding required for detector (a) is a boron tube plus ring [fig.5 No.9] to eliminate thermalized back scattered neutrons from carbon and hydrogen of the PE sphere. However, there is still the 11mm hole in the back end of the boron ring which could be covered with a boron disc having 4mm diameter hole at the center for the passage of the detector wire, but this component is smaller than 5% of Ri (fig.37) and it is negligible in comparison with the thermal neutron component of stray neutron fields.

For the PE sphere size it is desirable to have smaller possible one to decrease the weight of the system. However, small sphere sizes are not the best in giving lowest energy dependence to dose equivalent response for the quantity H_{MADE} [Rc]. In comparison with the 20cm and 30cm spheres figure 27

shows that Rc of the 25 cm sphere is of minimum energy dependence with monoenergetic fast neutrons in the energy range $1Ø^5$ to $1.5x1Ø^7$eV with a maximal variation of a factor of 1.8 However, what is more important is the combination of the Rc, Ri and Ra responses over the whole energy range which could give upon linear superposition the minimum variation in the indication of dose equivalent, absorbed dose and neutron flux. It is assumed from figure 38 that the 25 cm sphere gives less energy dependence for Rc and Ri (d=-6mm) combined, than the other spheres. This can be proved in future, after calibration of the sphere at 24keV, 2keV(1) and thermal neutrons and completion of the gap in the response by transport calculations. In any case, the heavy weight of the 3Øcm sphere (14 kg) plus the expected electronics, makes it inconvenient to use it as a portable neutron survey meter. Therefore, it is preferable to use the 25 cm sphere.

The minimum number of detectors required for the single sphere albedo system is three; the central detector (c), the albedo detector (i) and the thermal neutron detector (a). Since both Ri and Ra are directional dependent as shown in Fig.29 and Fig.31 where at the low neutron energies [57Ø keV to thermal] the ratio $Ri(18Ø^o)/Ri(Ø^o)$ drops to about 1Ø% and the ratio

---

(1) The source of neutrons which will be used to provide these energies is the PTB research reactor[11] .

Ri(rotation)/Ri(Ø°) increases to about 4Ø% (Fig.33)], therefore rotating the system improves directional dependence of the system by a factor of 4. Continues rotation of the system could be done either by advice fixed to the system or by putting the system on a rotating chair or table. The third alternative is to rotate the system manually every time by 9Ø° then add the four readings and divide by four. The rotating chair seems to be the best choice.

Using the sum of two opposite detector readings (see fig. 32) decreases the angular dependence by a factor of 5 for the 144keV and by higher factor for higher energies. However, adding a second albedo detector involves extra cost and weight to the system.

The work to be done in future involves building the necessary electronics and fixing a microprocesser to the system in order to get directly the readings of the neutron dose equivalent, absorbed dose and neutron flux. The energy response of the system over the whole neutron energy range (Ø--->15 MeV) has to be calculated after completing the calculation of the system response in the intermediate energies [Ø.4eV--->1ØØ KeV].

8. Field Calibration Technique for Personnel Albedo Dosimeters

We have seen in section 6 that for both active and passive detectors, the ratios Ri/Rc and Ra/Ri are correlated. These preliminary measurements were carried out in the stray neutron fields at DKFZ where the ratio i/a varies significantly over the different positions in the hall.

A graph was plotted to find the correlation between the ratio Ra/Ri for the active and passive detectors [fig.39]. This graph shows clearly that the two are correlated, they fit a straight line, except at the point in line with the neutron beam and very near to the accelerator target [position 99 in fig.10]. In this case, it is expected to observe significant difference between the two kinds of detectors.

For the final design of the active albedo system more measurements are required with the system together with passive albedo dosimeters in a stray neutron fields to establish calibration curve for the ratio Ra/Ri for the active detectors versus the same ratio Ra/Ri for the passive albedo dosimeter. This calibration curve is expected to be fixed for identical passive personnel albedo dosimeters.

In order to calibrate passive personnel dosimeters having (i) and (a) detectors in a particular nuclear facility, a neutron

survey has to be carried out with the active system to find, among others, the readings of the detectors (c), (i) and to establish a calibration curve Ri/Rc versus Ra/Ri for that facility.

Now we have two calibration curves, namely, (Ra/Ri) active versus (Ra/Ri) passive and Ri/Rc versus Ra/Ri for the active system. One could establish one calibration curve from these two curves that relates (Ri/Rc) active with Ra/Ri passive as a result of this one can find Rc for any a/i ratio of the passive albedo dosimeters.

9. Conclusion:

The aim of this project was, when submitted, to investigate field calibration techniques for personnel neutron dosimeters. However, it was expanded to the developing of an active single sphere albedo system for the measurement of neutron dose equivalent rates and field calibratin of personnel neutron dosimeters using three ^{3}He proportional counters in a polyethelene sphere. One is located at the center to measure neutron dose equivalent and the other two near the surface, simulating the albedo personnel dosimeter, one to measure albedo neutron response and the second to measure thermal neutron response as explained earlier.

The response of the central, albedo and thermal detectors of the system was investigated experimentally in the following neutron energies: thermal, Ø.144, Ø.25Ø, Ø.57Ø, 1.2, 2.5, 5.5, and 14.8 MeV and Cf-252 neutrons.

The experimental measurements revealed the following:

For the central detector "C", which measures the neutron dose equivalent, the response was angular independent, but energy dependent [Fig.27]. The 25cm PE sphere showed the lowest energy dependence of 45% maximal variation in the fast neutron energy

range. It is expected that the linear superposition of the readings of the central detector with the albedo detector and the thermal detector will minimize the energy dependence of the central detector. In the case of a neutron spectrum, the energy response of the central detector will become smoother as compared with that of monoenergetic neutrons, because, in this case, extreme values of the response will average out.

For the albedo detector (i) the response was highly energy and angular dependent as shown in Fig.29 and Fig.30 respectively. For example, the energy dependence of the 25cm PE sphere in the fast energy range varied by a factor of ten. This variation was relatively lower for higher detector's depth as shown in Figure 31.

The angular dependence was more significant at the lower energy range. It could vary by a factor of ten [Fig.35 and 36]. Rotating the system reduced the angular dependence by upto a factor of four [Fig.33]. Using the sum of two opposite albedo detector readings [Fig.32] reduces the angular dependence better. However, this involves using two albedo counters which increases the cost and the weight of the system.

For the thermal detector (a), the response followed similar pattern in energy dependence in the fast neutron energy range like the albedo detector response [Fig.37]. The ratio of the albedo detector response in this energy range was constant and equal to Ø.Ø5.

It was found that albedo response normalized to the reference value of the dose equivalent [Ri/Rc] versus reading ratio [Ra/Ri] correlated [i.e., fits a straight line] in a stray neutron field [Fig.38]. Similar results was found with thermoluminescent detectors [i.e. passive detectors] in the single sphere albedo system [Fig.37].

It was also found that the ratio Ra/Ri for the active and the passive detectors correlated [i.e., fits a straight line] in the same stray neutron field [Fig.40]. This correlation will enable the calibration of the albedo personnel dosimeters to find the dose equivalent from the reading ratio (a/i) using the calibration curve of Ri/Rc versus Ra/Ri of the active system and the second calibration curve of $(Ra/Ri)_{active}$ versus $(Ra/Ri)_{passive}$.

A theoretical calculation is being worked out to find the system response in the intermediate neutron energy range, Ø.4 eV to 1 KeV, to fill the gap in the experimental measurements.

The overall energy response of the system in terms of the neutron dose equivalent, the absorbed dose and the neutron flux will be evaluated over the whole energy range, Ø.ØØ25 eV to 15 MeV, upon finishing the theoretical calculation mentioned earlier.

The active albedo system will be used upon completion to give the readings of neutron dose equivalent, absorbed dose and neutron flux in nuclear facilities by linear superposition of the three detector readings [i.e., c, i and a] using a microprocessor. It will also be used to find calibration factors for the neutron personnel albedo dosimeters particularly those having two thermal detectors, like TLD's, to measure albedo and thermal neutron components.

REFERENCES

1. J. Gibson and E. Piesch Neutron Monitoring for Radiological Protection, IAEA Technical Report Series No. 252, (1985).

2. H. Lesiecki and M. Cosack, "Response of Neutron Dose Equivalent Survey Meters. 1st Symposium on Personnel Radiation Dosimetry" Knoxville, Tennessee (1985), not published.

3. Ing H. and Piesch E. Status of Neutron Dosimetry, Radiat. Prot. Dosim. Vol. 10 No. 1-4, p.5 (1985).

4. Piesch E. Calibration technique for personnel dosimetry in stray neutron fields, Radiat. Prot. Dosim. Vol. 10 No. 1-4, p. 159 (1985).

5. Piesch E. Burgkhardt B. and Comper W. The single sphere Albedo System- A useful technique in Neutron Dosimetry, Radiat. Prot. Dosim. Vol 10 No. 1-4, p. 147 (1985).

6. Piesch E. and Burgkhardt, B., Albedo Neutron Dosimetry Rad. Prot. Dos. Vol 10 No. 1-4, p. 175 (1985).

7. Siebert and Hollnagel, Intercomparison and evaluation of calculated Neutron Fluence to ambient Dose Equivalent conversion factors. Radiat. Prot. Dosim. Vol.12 No.2, p. 145 (1985)

8. ICRU 39, Determination of Dose Equivalent Resulting from External Radiation Sources. Report 39 (Bethesda, MD: ICRU Publications) (1985).

9. Schraube, H. GSF report No. 465 (1974).

10. G.F. Knoll, Radiation Detection and Measurement, John Wiley, (1979).

11. Piesch, Burgkhardt and Hofmann, Calibration of Neutron Detectors in Radiation Protection, KfK report No. 2847, Sept. (1979).